Article

Reactions of Vinyl Acetate and Vinyl Trifluoroacetate with Cationic Diimine Pd(II) and Ni(II) Alkyl Complexes: Identification of Problems Connected with Copolymerizations of These Monomers with Ethylene

B. Scott Williams, Mark D. Leatherman, Peter S. White, and Maurice Brookhart

J. Am. Chem. Soc., **2005**, 127 (14), 5132-5146• DOI: 10.1021/ja045969s • Publication Date (Web): 17 March 2005

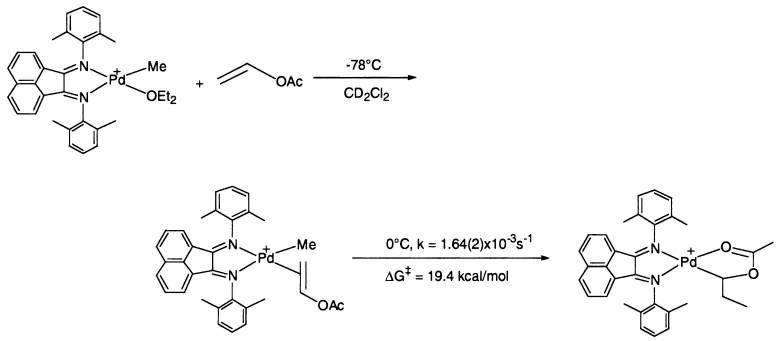

More About This Article

Additional resources and features associated with this article are available within the HTML version:

- Supporting Information
- Links to the 7 articles that cite this article, as of the time of this article download
- Access to high resolution figures
- Links to articles and content related to this article
- Copyright permission to reproduce figures and/or text from this article

View the Full Text HTML

J|A|C|S
ARTICLES
Published on Web 03/17/2005

Reactions of Vinyl Acetate and Vinyl Trifluoroacetate with Cationic Diimine Pd(II) and Ni(II) Alkyl Complexes: Identification of Problems Connected with Copolymerizations of These Monomers with Ethylene

B. Scott Williams, Mark D. Leatherman, Peter S. White, and Maurice Brookhart*

Contribution from the University of North Carolina, Department of Chemistry CB 3290, Venable Hall, Chapel Hill, North Carolina 27599-3290

Received July 6, 2004; E-mail: mbrookhart@unc.edu

Abstract: Vinyl acetate (VA) and vinyl trifluoroacetate (VA_f) react with [(N∧N)Pd(Me)(L)][X] (M = Pd, Ni, (N∧N) = *N,N′*-1,2-acenaphthylenediylidene bis(2,6-dimethyl aniline), Ar_f = 3,5-trifluoromethyl phenyl, L = Ar_fCN, Et_2O; X = $B(Ar_f)_4^-$, SbF_6^-) to form π-adducts **3** and **5** at −40 °C. Binding affinities relative to ethylene have been determined. Migratory insertion occurs in a 2,1 fashion ($\Delta G^{\ddagger}$ = 19.4 kcal/mol, 0 °C for VA, and 17.4 kcal/mol, −40 °C for VA_f) to yield five-membered chelate complexes [(N∧N)Pd(κ^2-CH(Et)(OC(O)-CH_3))]$^+$, **4**, and [(N∧N)Pd(κ^2-CH(Et)(OC(O)CF_3))]$^+$, **6**. When VA is added to [(N∧N)Ni(CH_3)]$^+$, an equilibrium mixture of an η^2 olefin complex, **8c**, and a κ-oxygen complex, **8o**, results. Insertion occurs from the η^2 olefin complex, **8c** ($\Delta G^{\ddagger}$ = 15.5 kcal/mol, −51 °C), in both a 2,1 and a 1,2 fashion to generate a mixture of five- and six-membered chelates, $\mathbf{9_{2,1}}$ and $\mathbf{9_{1,2}}$. VA_f inserts into the Ni−CH_3 bond (−80 °C) to form a five-membered chelate with no detectable intermediate. Thermolysis of the Pd chelates results in β-acetate elimination from **4** ($\Delta G^{\ddagger}$ = 25.5 kcal/mol, 60 °C) and β-trifluoroacetate elimination from **6** ($\Delta G^{\ddagger}$ = 20.5 kcal/mol, 10 °C). The five-membered Ni chelate, $\mathbf{9_{2,1}}$, is quite stable at room temperature, but the six-membered chelate, $\mathbf{9_{1,2}}$, undergoes β-elimination at −34 °C. Treatment of the OAc_f containing Pd chelate **6** with ethylene results in complete opening to the π-complex [(N∧N)Pd(κ^2-CH(Et)(OAc_f))(CH_2CH_2)]$^+$ (OAc_f = $OC(O)CF_3$), **18**, while reaction of the OAc containing Pd chelate **4** with ethylene establishes an equilibrium between **4** and the open form **16**, strongly favoring the closed chelate **4** (ΔH = −4.1 kcal/mol, ΔS = −23 eu, K = 0.009 M^{-1} at 25 °C). The open chelates undergo migratory insertion at much slower rates relative to those of the simple (N∧N)Pd(CH_3)(CH_2CH_2)$^+$ analogue. These quantitative studies provide an explanation for the behavior of VA and VA_f in attempted copolymerizations with ethylene.

Introduction

The study of late transition metal olefin polymerization catalysis has advanced remarkably in recent years.[1] A primary motivating factor for the development of such catalysts is that the late metals are less oxophilic than early metals and, hence, more compatible with functionalized olefins. Of particular interest is the copolymerization of ethylene with polar vinyl monomers. It has been demonstrated that the palladium diimine complexes [(N∧N)PdMe(L)][$B(Ar_f)_4$] ((N∧N) = *N,N′*-1,2-acenaphthylenediylidene bis(2,6-dimethyl aniline), L = $NCAr_f$ (Ar_f = 3,5-$(CF_3)_2C_6H_3$), **1**; L = Et_2O, **2a**) are active catalysts for the polymerization of ethylene[2−4] and are capable of copolymerizing ethylene and methyl acrylate (MA).[4] However, turnover frequencies in copolymerizations are greatly reduced relative to ethylene homopolymerization, making use of these catalysts commercially impractical. Recently, the DuPont group has developed similar copolymerizations using an analogous nickel catalyst operating at high temperature.[5] However, the vast majority of potential polar vinyl comonomers have remained intractable.[1] While some unsaturated species are simply not incorporated into a copolymer but do not interfere with ethylene homopolymerization, others (such as vinyl nitriles, vinyl halides, and vinyl acetate) shut down polymerization activity. In the case of vinyl nitriles, the nitrile functionality binds directly to the active polymerization site of palladium, while, for vinyl halides, β-halide elimination from the growing polymer chain generates unreactive metal halide dimers.[6,7] However, in the case of vinyl acetate (VA), the mechanism of inhibition has yet to be explored.

(1) (a) Ittel, S. D.; Johnson L. K.; Brookhart, M. *Chem. Rev.* **2000**, *100*, 1169 and references therein. (b) Gibson, V. C.; Spitzmesser, S. K. *Chem. Rev.* **2003**, *103*, 283 and references therein.
(2) The designations **a** and **b** are used throughout to distinguish identical cationic complexes paired with $B(Ar_f)_4^-$ and SbF_6^- counterions, respectively. In cases where only one of the two salts was prepared, **a** and **b** are omitted.
(3) Tempel, D. J.; Johnson, L. K.; Huff, R. L.; White, P. L.; Brookhart, M. *J. Am. Chem. Soc.* **2000**, *122*, 6686.
(4) Mecking, S.; Johnson, L. K.; Wang, L.; Brookhart, M. *J. Am. Chem. Soc.* **1998**, *120*, 888.
(5) (a) *Polym. Mater. Sci. Eng.* **2002**, *86*, 319. (b) *Polym. Mater. Sci. Eng.* **2002**, *86*, 320−321
(6) (a) Kang, M.; Sen, A.; Zakharov, L.; Rheingold, A. L. *J. Am. Chem. Soc.* **2002**, *124*, 12080. (b) Schultz, L. H.; Brookhart, M. Unpublished results.
(7) (a) Foley, S. R.; Stockland, R. A., Jr.; Shen, H.; Jordan, R. F. *J. Am. Chem. Soc.* **2003**, *125*, 4350. (b) Shen, H.; Jordan, R. F. *Organometallics* **2003**, *125*, 4350.

10.1021/ja045969s CCC: $30.25

Scheme 1. Formation of VA and VA_f Chelates

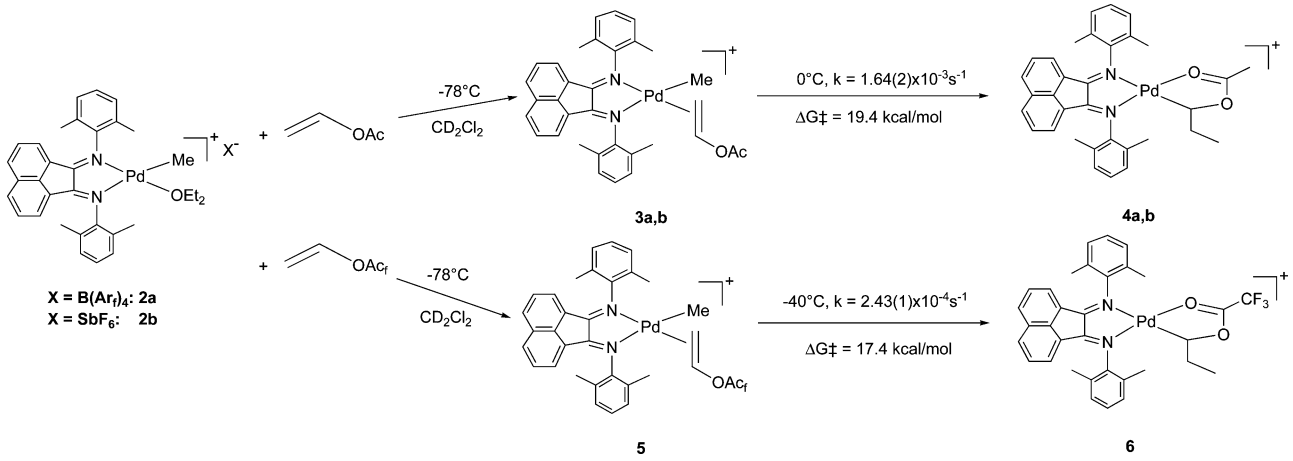

Understanding the behavior of VA is necessary if catalysts are to be modified in a manner which may enable ethylene/VA copolymerization. We report here a detailed study of the reactions of VA and related unsaturated acetates with Ni and Pd diimine complexes, which provides fundamental information regarding insertion barriers of these monomers, their binding affinities relative to ethylene, the nature and stability of the insertion products, and the propensity of these inserted species to incorporate further equivalents of monomer. This body of information provides significant insight into the problems of employing vinyl acetate and related comonomers in ethylene copolymerizations.

Results

Low-Temperature Generation of π-Olefin Complexes and Insertion into the M−Me Bond. Addition of vinyl acetate (VA) to the cationic palladium complex $[(N\wedge N)PdMe(OEt_2)][B(Ar_f)_4]$ (**2a**) at −78 °C results in the quantitative release of ether and formation of a new complex, $[(N\wedge N)PdMe(\eta^2\text{-}(C_2H_3)O_2CCH_3)][B(Ar_f)_4]$ (**3a**) (Scheme 1). The ^{1}H NMR signals of the methylidene protons appear upfield (δ = 4.05, 4.20) of those for free VA (δ = 4.60, 4.91), consistent with an η^2-olefinic complex rather than an O-bound complex.[4] Similarly, the methylidene carbon of the olefin moiety appears at 67.8 ppm in the ^{13}C NMR spectrum (δ = 98.3 ppm in free VA), fully consistent with an η^2-olefin complex.

Upon cooling to −105 °C in $CDCl_2F$, these signals separate into two pairs (major δ = 4.27 (br d, 16 Hz), 3.85 (br s); minor δ = 4.17 (br s), 3.70 (br d, 14 Hz)), presumably due to static rotamers of the olefin complex.[8] When the temperature is raised to −20 °C, the olefin inserts cleanly into the Pd−C bond in a 2,1 fashion, resulting in the formation of a chelate complex, $[(N\wedge N)PdMe(\kappa^2\text{-}CH(OAc)Et)][B(Ar_f)_4]$ (**4a**). Goddard et al. have predicted a strong preference ($\Delta\Delta G^{\ddagger}$ = 3.3 kcal/mol) for 2,1 insertion of vinyl acetate over 1,2 insertion.[9] This insertion reaction is very similar to one reported by Liu et al.,[10] in which vinyl acetate was found to insert into a palladium methyl bond to form an analogous chelate. The hexafluoroantimonate salt $[(N\wedge N)PdMe(OEt_2)][SbF_6]$ (**2b**) reacts in a similar fashion with vinyl acetate to form **3b** (Scheme 1) and subsequently the chelate **4b**. The insertion reaction is first-order in palladium and displays clean kinetic behavior. Figure 1 shows an Eyring plot for this insertion reaction over the range −40° to 0 °C in CD_2Cl_2. From these data, values of $\Delta H^{\ddagger}$ = 20.2(1.3) kcal/mol and $\Delta S^{\ddagger}$ = 3(5) eu were obtained. At 0 °C, $k = 1.64(2) \times 10^{-3}$ s^{-1} and $\Delta G^{\ddagger}$ = 19.4(1) kcal/mol. The corresponding vinyl trifluoroacetate ($CH_2CHO_2CCF_3$, VA_f) complex, $[(N\wedge N)PdMe(\eta^2\text{-}C_2H_3(OAc_f))][SbF_6]$ (**5**, $OAc_f = O_2CCF_3$) can be similarly generated from **2b** and VA_f. **5** displays similar spectral features to the vinyl acetate analogue **3**, including the upfield shift of the methylidene olefinic protons (4.18 and 4.66, relative to 5.17 and 4.89 in the free olefin) and the broadening of the signals at low temperature due to slow rotation. However, the signals of **5** do not decoalesce at accessible temperatures. Upon warming to −40 °C the VA_f moiety inserts into the Pd−C bond with $k_{obs} = 2.43(1) \times 10^{-4}$ s^{-1} ($\Delta G^{\ddagger}$ = 17.4(1) kcal/mol) to afford the chelate complex $[(N\wedge N)PdMe(\kappa^2\text{-}CH(OAc_f)Et)][SbF_6]$ (**6**). At the same temperature, the insertion barrier for vinyl acetate is calculated to be 19.5 kcal/mol (see above). This is in keeping with the perception of olefin insertion as a nucleophilic attack by the palladium alkyl upon the coordinated olefin; electron-withdrawing groups increase the electrophilicity of the olefinic group.

When the analogous nickel cation $[(N\wedge N)NiMe(OEt_2)][B(Ar_f)_4]$ (**7**) is exposed to ca. 2 equiv of VA at −80 °C in $CDCl_2F$, ≥90% of the ether is displaced to form a new complex, $[(N\wedge N)NiMe(C_2H_3OAc)][B(Ar_f)_4]$ (**8**) (Scheme 2). The two methylidene signals remain broad under these conditions, but upon lowering the temperature to −120 °C, they separate into two pairs of signals in a 9:1 ratio (ΔG = 0.7 kcal/mol). The lesser of these is strongly shielded (δ = 3.82, 4.06) and is assigned to the η^2-olefin complex, **8c**, with a Ni−Me signal at −0.61 ppm, while the major product (δ = 4.5, 4.7, partially obscured by free olefin) is assigned to the O-bound isomer, **8o** with a Ni−Me signal at −0.26 ppm. Ziegler[11] has predicted that the Olefin-bound isomer should be preferred over the O-bound isomer by over 5 kcal/mol for palladium, yet the O-bound species is expected to be 0.7 kcal/mol more favorable for nickel. Both predictions are in excellent agreement with our results. Upon warming to −51 °C, **8** undergoes insertion (k_{obs} = 5.5 ×

(8) Similar pairs are observed for coordinated propylene, though the rotation cannot be completely frozen out in this case.
(9) Phillip, D. M.; Muller, R. P.; Goddard, W. A., III.; Storer, J.; McAdon, M.; Mullins, M. *J. Am. Chem. Soc.* **2002**, *124*, 10198.
(10) (a) Reddy, K. R.; Chen, C.-L.; Liu, Y.-H.; Peng, S.-M.; Chen, J.-T.; Liu, S.-T. *Organometallics* **1999**, *18*, 2574. (b) Reddy, K. R.; Surekha, K.; Lee, G.-H.; Peng, S.-M.; Chen, J.-T.; Liu, S.-T. *Organometallics* **2001**, *20*, 1292.
(11) Michalak, A.; Ziegler, T. *Organometallics* **2001**, *20*, 1521.

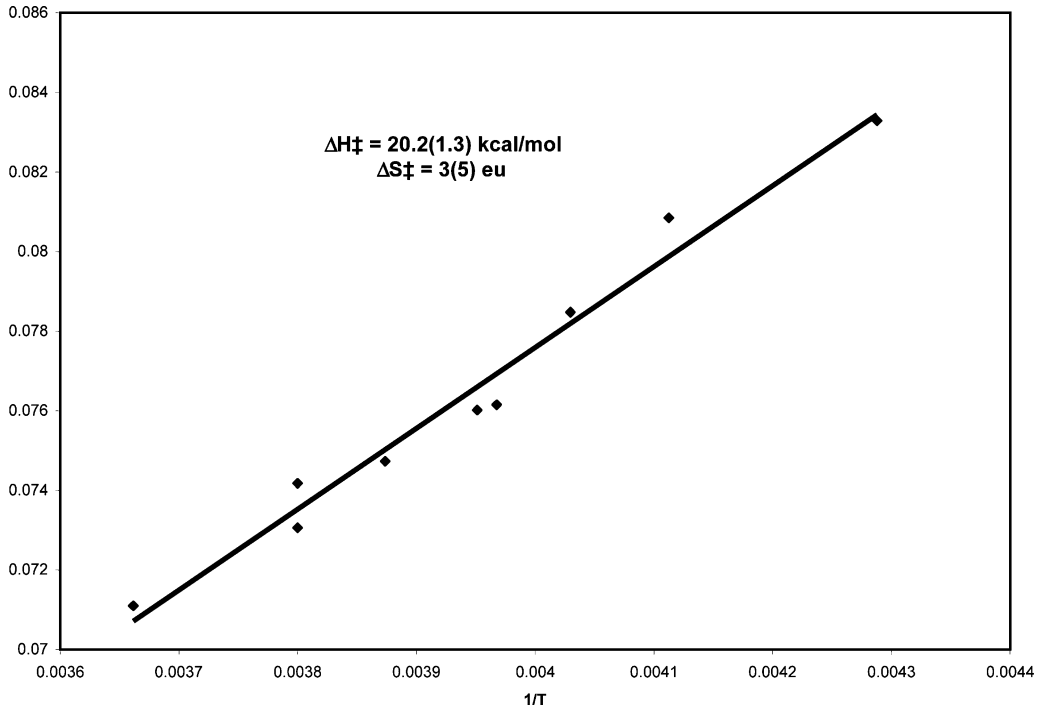

Figure 1. Eyring Plot of VA Insertion into Pd−Me Bond of **3b** From −40 °C to 0 °C.

Scheme 2. Insertion Mechanism for the Nickel VA Complex **3c**

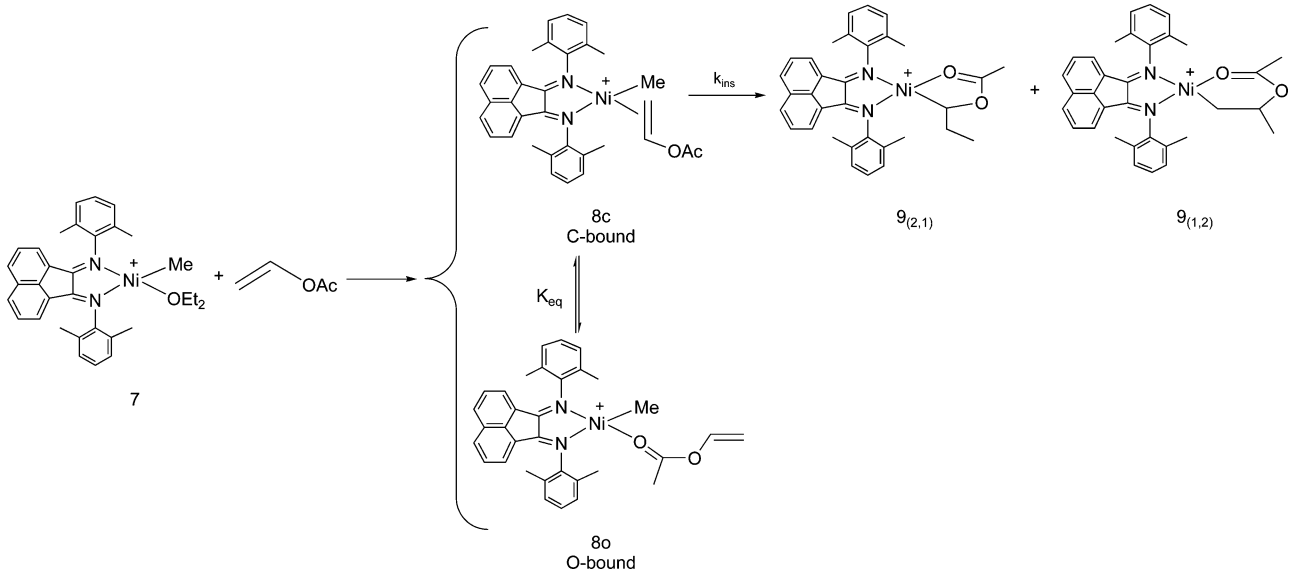

10^{-4} s^{-1} for the disappearance of **8** (**8c** plus **8o**)) to form two species, [(N∧N)Ni(κ^2-CH(Et)(OAc))][B(Ar_f)$_4$] (**9$_{(2,1)}$**) and [(N∧N)-Ni(κ^2-CH_2CH(Me)(OAc))][B(Ar_f)$_4$] (**9$_{(1,2)}$**) in roughly a 2:1 ratio, resulting from 2,1 and 1,2 insertion, respectively. Since insertion presumably proceeds from **8c**, $k_{obs} = K_{eq}k_{ins}$, where K_{eq} represents the **8c:8o** equilibrium (Scheme 2) in which the latter is disfavored by ca. 0.7 kcal/mol ($K_{eq} = 0.20$), and thus k_{ins} can be estimated at ca. 3×10^{-3} s^{-1} ($\Delta G^{\ddagger} = 15.5$ kcal/mol).[12]

In contrast, addition of VA_f to **7** at −80 °C results in rapid formation of [(N∧N)Ni(κ^2-CH(Et)(OAc_f))][B(Ar_f)$_4$] (**10**) with no intermediate being detectable. Either displacement of ether is rate determining or there is a rapid preequilibrium established between **7** (favored) and the VA_f adduct. The reaction proceeds much more rapidly in the presence of a higher concentration of VA_f, consistent with either mechanism. A value of $k_{obs} = 1.6 \times 10^{-4}$ M^{-1} s^{-1} was obtained for the overall reaction at −40 °C, corresponding to a $\Delta G^{\ddagger} = 17.3(1)$ kcal/mol. This value is an upper limit to the true insertion barrier.

Synthesis and Characterization of Chelates from Insertion of Unsaturated Acetates. Addition of VA to [(N∧N)PdMe-(NCAr$_f$)][B(Ar$_f$)$_4$] (**1**) at 0 °C results in quantitative formation of [(N∧N)PdMe(κ^2-CH(OAc)Et)][B(Ar$_f$)$_4$] (**4a**), but this complex is an oily solid and difficult to obtain in crystalline form. For this reason, we prepared the analogous SbF_6^- salt, [(N∧N)-Pd(κ^2-CH(OAc)(Et))][SbF_6] (**4b**), by reaction of (N∧N)PdMeCl with $AgSbF_6$ in methylene chloride at −78 °C, followed by

(12) This rate represents both 2,1 and 1,2 insertion. By the Curtin−Hammett principle, the ratio of rates is equal to the ratio of the products, and thus $k_{2,1} \approx 2 \times 10^{-3}s^{-1}$ and $k_{1,2} \approx 1 \times 10^{-3}s^{-1}$, corresponding to $\Delta G^{\ddagger}$ values of 15.6 and 15.9 kcal/mol, respectively.

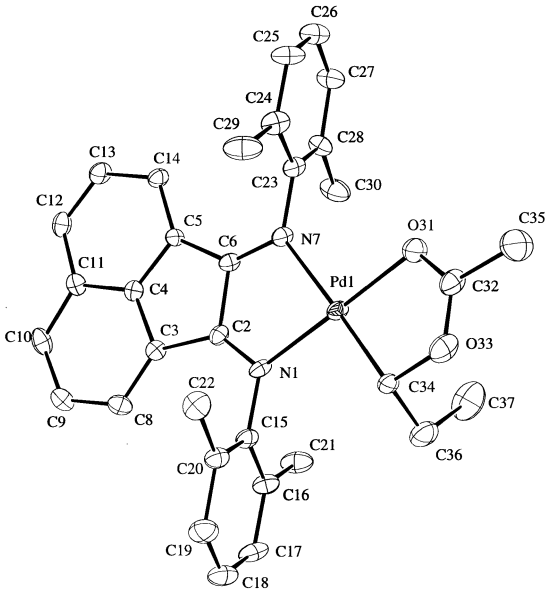

Figure 2. ORTEP of **4b**. Selected Bond Lengths (Å): Pd(1)−N(1), 2.061(6); Pd(1)−N(7), 2.148(6); Pd(1)−O(31), 2.035(5); Pd(1)−C(34), 2.001(7); O(33)−C(34), 1.474(9); C(32)−O(33), 1.281(11); O(31)−C(32), 1.260(10). Selected Angles (deg): N(1)−Pd(1)−N(7), 80.19(22); O(31)−Pd(1)−C(34), 81.4(3); Pd(1)−C(34)−C(36), 114.4(6); Pd(1)−C(34)−O(33), 106.9(6); N(1)−Pd(1)−C(34), 98.2(3); N(7)−Pd(1)−O(31), 100.05(22).

addition of VA and gradual warming to room temperature. X-ray quality crystals of **4b** were grown from slow diffusion of pentane into a dichloromethane solution. An ORTEP view is shown in Figure 2. Table 2 (Experimental Section) contains important structural parameters.

The most interesting feature of this structure is that the formal carbon−oxygen single (C_{32}—O_{33}) and double (C_{32}—O_{31}) bonds are very similar in length (1.281(11) and 1.260(10) Å, respectively; $\Delta = 0.021(15)$ Å), more closely resembling the bond lengths of a carboxylate anion (1.254(1) Å) than those of an aliphatic ester (1.19 and 1.34 Å, $\Delta = 0.15$ Å).[13] Liu et al. have reported the structural characterization of a similar chelate species supported by a P∧N ligand, *o*-(diphenylphosphino)-*N*-benzaldimine.[10] In their structure, the oxygen is trans to the stronger donor phosphorus, and the Pd—O bond is consequently 0.053(9) Å longer, and the C═O bond is 0.05(2) Å shorter than the corresponding bonds in **4b**. The carboxylate C—O single bond and Pd—C bond lengths are effectively identical in the two structures.

While insertion of VA into the Pd−Me bond of **3** proceeds exclusively in a 2,1 fashion to afford **4**, reaction of allyl acetate with (N∧N)PdMeCl in the presence of $AgSbF_6$ affords a mixture of [(N∧N)PdMe(κ^2-CH(OAc)*i*Pr)][SbF_6] (**11**$_{(1,2)}$) (resulting from 1,2 insertion) and [(N∧N)PdMe(κ^2-CH(OAc)*n*Pr)][SbF_6] (**11**$_{(2,1)}$) (resulting from 2,1 insertion) in a ratio of roughly 1:2 (Scheme 3). After insertion, the palladium undergoes "chain running" via β-hydride elimination/ reinsertion reactions, to migrate to the carbon α to acetate whereupon a chelate forms.

Similarly, reaction of (N∧N)PdMeCl with 3-butenyl acetate in the presence of $AgSbF_6$ results in a ∼1:2 mixture of [(N∧N)-PdMe(κ^2-CH(OAc)*i*Bu)][SbF_6] (**12**$_{(1,2)}$) from 1,2-insertion and [(N∧N)PdMe(κ^2-CH(OAc)*n*Bu)][[SbF_6] (**12**$_{(2,1)}$) from 2,1 insertion (Scheme 4). Similar mixtures of 1,2 and 2,1 insertion products are typical for α-olefins with these catalysts.[14] Since the pairs of isomers **11**$_{(2,1)/(1,2)}$ and **12**$_{(2,1)/(1,2)}$ are generated together and have very similar structures, we were generally unable to separate these complexes, but pure **11**$_{(2,1)}$ (R = *n*Pr) was obtained by crystallization from a THF/diethyl ether solution of **11**$_{(2,1)}$ and **11**$_{(1,2)}$ and Pasteur separation of the orange plates (**11**$_{(2,1)}$) from the yellow microcrystals (**11**$_{(2,1)/(1,2)}$ mixture).

The most unusual spectral feature of this class of complexes is the surprisingly high field chemical shift of the proton and carbon (5.50 and 105.5 ppm, respectively, for **4a** in CD_2Cl_2) α to the acetate group. The two protons β to the acetate in **4a** are diastereotopic and appear as complex multiplets at 0.87 and 1.15 ppm, while the γ-methyl group appears as a broad triplet at 1.07 ppm. The products of allyl acetate (**11**$_{(1,2)}$, R = *i*Pr; **11**$_{(2,1)}$, R = *n*Pr, Scheme 3) and 3-butenyl acetate insertion (**12**$_{(1,2)}$, R = *i*Bu; **12**$_{(2,1)}$, R = *n*Bu, Scheme 4) could be identified by 2D NMR spectroscopy and exhibit spectral features similar to those of **4**. The related nickel complex [(N∧N)NiMe(CH(OAc)Et)]-[$B(Ar_f)_4$] (**9**$_{2,1}$) was prepared and isolated by a method analogous to that of **4** and is stable at room temperature.

To prepare chelate complexes which might more easily open to form monodentate species, we investigated the reaction of isopropenyl acetate and VA_f with (N∧N)PdMeCl in the presence of $AgSbF_6$ (Scheme 4). In the case of isopropenyl acetate, exclusive 2,1 insertion afforded the complex [(N∧N)Pd(κ^2-C(OAc)(Me)(Et))][SbF_6] (**13**), which contains a tertiary carbon bound to palladium. Reaction with VA_f at −78 °C, followed by warming to −20 °C generated the expected chelate [(N∧N)-Pd(κ^2-CH(OAc_f)Et)][SbF_6] (**6**, Scheme 1), but it was necessary to crystallize and isolate this complex at low temperature, as it decomposes at room temperature in solution. The corresponding nickel complex was not isolable.

Thermal Stability of Palladium Chelate Complexes. As indicated, the trifluoroacetato complex [(N∧N)Pd(κ^2-CH(OAc_f)-Et)][SbF_6] (**6**) is unstable at room temperature, generating propylene and a mixture of palladium decomposition products (Scheme 5). All of the other chelates (**4**, **11**−**13**) decompose in a similar fashion at higher temperatures, affording the corresponding olefin (propylene for **4** and **13**, butenes for **11**, pentenes for **12**).

The initial palladium-containing decomposition products are dominated by a highly symmetric species with only a single signal for the aryl methyl groups of the (N∧N) ligand. These initial products are tentatively assigned as [(N∧N)Pd(κ^2-O_2CR)]$^+$ (R = CH_3, CF_3); however, as they are never cleanly formed under the reaction conditions and themselves decompose to form mixtures of several species, a complete characterization has not been pursued. We assume that these decompositions occur via β-acetate elimination reactions (see below). The key factor for purposes of understanding catalytic activity is the stability of the starting material, as decomposition of the catalyst will obviously result in concomitant loss of catalytic activity, regardless of the precise nature of these decomposition products. In all cases, the decomposition was cleanly first-order in palladium starting material. Table 1 lists first-order rate constants for decomposition of the various chelate complexes and the corresponding $\Delta G^{\ddagger}$ values. With the exception of [(N∧N)Pd-(κ^2-CH(OAc)*i*Pr)][SbF_6] (**11**$_{(1,2)}$), [(N∧N)Pd(κ^2-CH(OAc_f)Et)]-[SbF_6] (**6**), and the nickel complex [(N∧N)Ni(κ^2-CH(OAc_f)-Et)][SbF_6] (**10**) (vide infra), all thermolyses were carried out at

(13) Allen, F. H.; Kennard, O.; Watson, D. G.; Brammer, L.; Orpen, A. G.; Taylor, R. *J. Chem. Soc., Perkin Trans. 2* **1987**, S1−S19 (follows p 1914).

Scheme 3. Insertion of Allyl Acetate into the Palladium−Methyl Bond

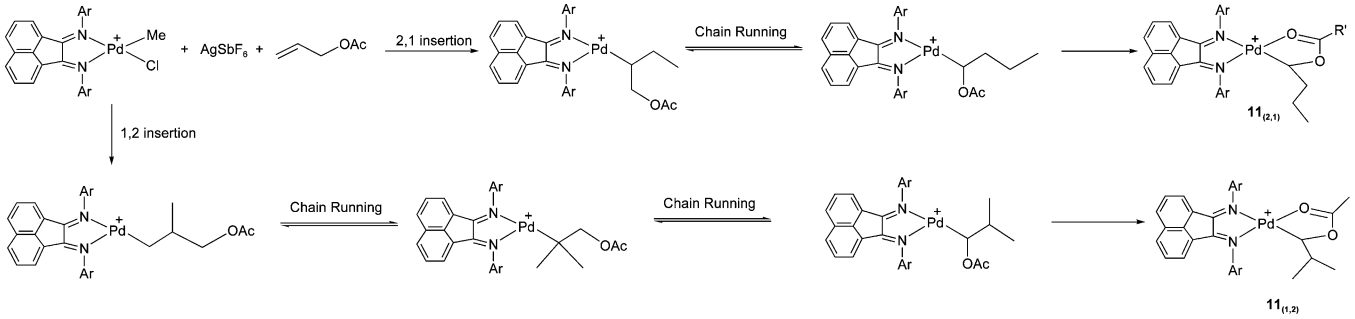

Scheme 4. Insertion of Other Unsaturated Acetates into the Palladium−Methyl Bond

Scheme 5. Decomposition of Acetate Chelates of Nickel and Palladium

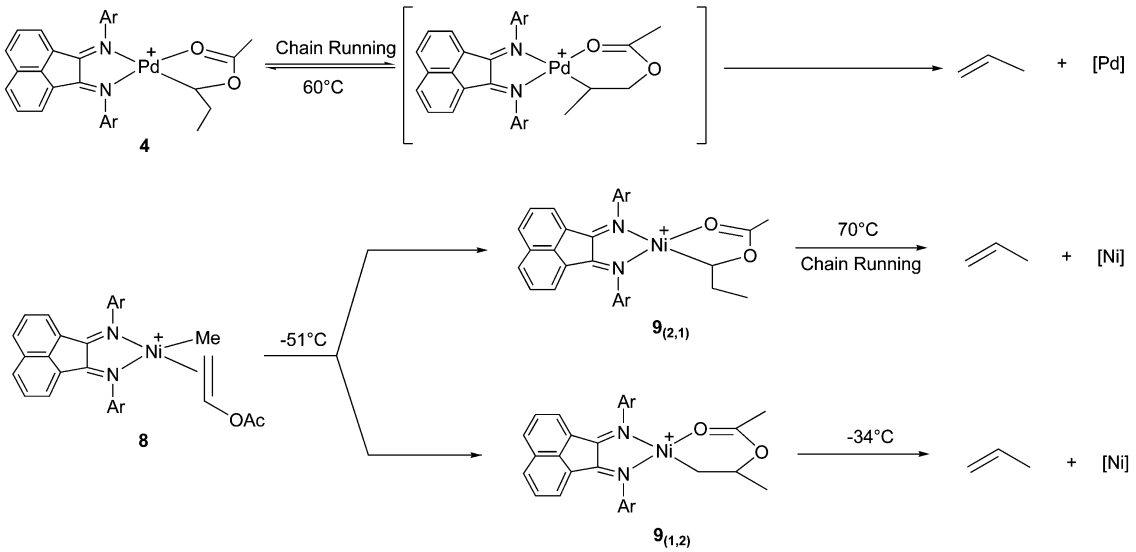

60 °C. Since these latter two complexes were not thermolyzed at the same temperatures, the free energies of activation are not directly comparable but are certainly informative in a relative sense. Complexes **4** and **11**−**13** are all stable for extended periods at room temperature in solution and are thus stable under typical polymerization conditions.

Stability of Nickel Chelate Complexes. Reaction of [(N∧N)-NiMe(OEt_2)][$B(Ar_f)_4$] with vinyl acetate results in both 2,1 and 1,2 insertion to afford the five-membered chelate [(N∧N)Ni-(CH(Et)(OAc))][$B(Ar_f)_4$] (**9**$_{(2,1)}$) (Scheme 5) and the six-membered chelate [(N∧N)Ni(CH_2CH(Me)(OAc))][$B(Ar_f)_4$] (**9**$_{(1,2)}$), respectively. Complex **9**$_{(1,2)}$ contains an acetate group β to nickel and reacts at −34 °C to form propylene and paramagnetic nickel products ($k_{obs} = 2.87 \times 10^{-4}$ s^{-1}, $\Delta G^{\ddagger} = 17.7$ kcal/mol), while **9**$_{(2,1)}$ decomposes at much higher temperatures (>70 °C) to afford similarly intractable products. By way of contrast, VA_f inserts exclusively 2,1 to yield [(N∧N)Ni(CH(Et)(OAc_f))]-[$B(Ar_f)_4$] (**10**), which decomposes to form propylene and nickel products at 40 °C ($k_{obs} = 1.58 \times 10^{-4}$ s^{-1}, $\Delta G^{\ddagger} = 23.8$ kcal/mol). The slightly greater stabilities of the nickel complexes

Scheme 6. Reaction of **4** with Acetonitrile and Subsequent Rearrangement

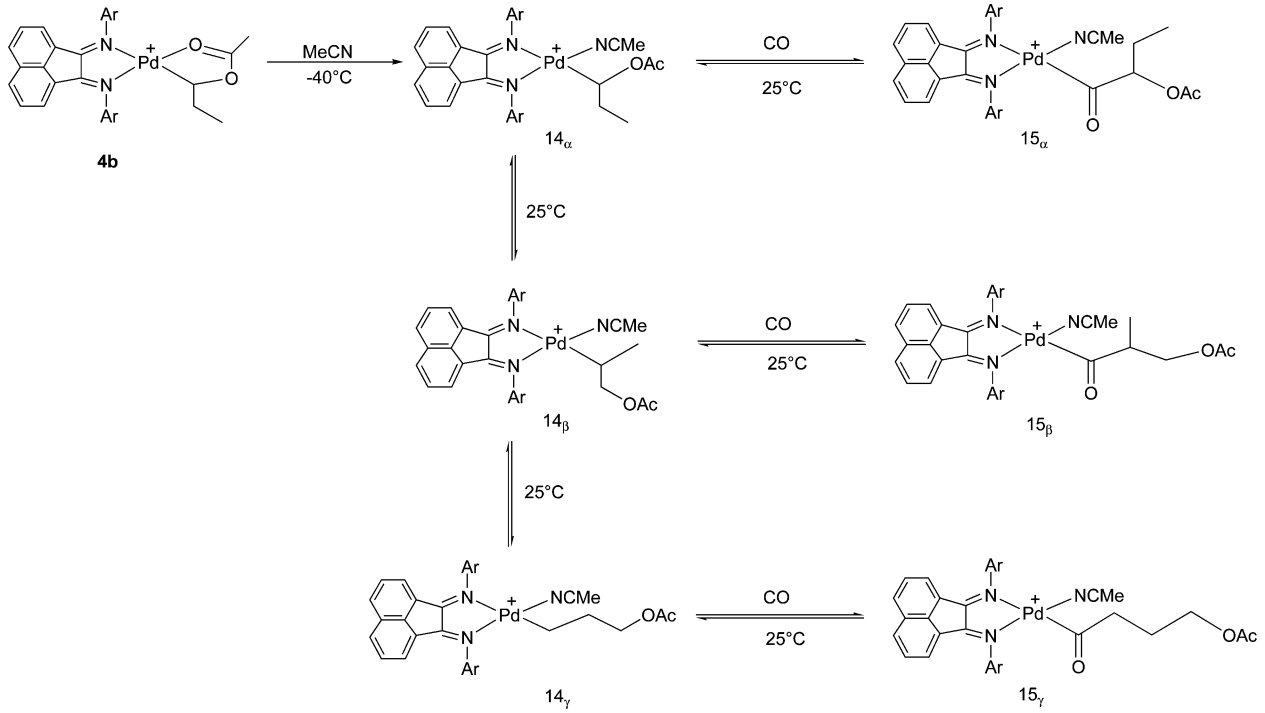

Table 1. Thermolyses of [(N∧N)M(C(R)(R′)(O$_2$CR″))][X] in $C_2D_2Cl_4$

compound	M	R	R′	R″	X$^-$	*T* (°C)	k_{obs} (×10^4 s^{-1})	$\Delta G^{\ddagger}$ (kcal/mol)
4a	Pd	Et	H	Me	$B(Ar_f)_4$	60	1.29(2)	25.5
4b	Pd	Et	H	Me	SbF_6	60	1.25(3)	25.5
6[a]	Pd	Et	H	CF_3	SbF_6	10	8.13(3)	20.5
10	Ni	Et	H	CF_3	$B(Ar_f)_4$	40	1.58(2)	23.8
11$_{(2,1)}$	Pd	*n*Pr	H	Me	SbF_6	60	1.33(3)	25.5
11$_{(1,2)}$	Pd	*i*Pr	H	Me	SbF_6	120	2.42(6)	29.7
12$_{(2,1)}$	Pd	*n*Bu	H	Me	SbF_6	60	1.35(2)	25.5
12$_{(1,2)}$	Pd	*i*Bu	H	Me	SbF_6	60	0.97(1)	25.7
13	Pd	Et	Me	Me	SbF_6	60	3.49(3)	24.8

[a] In CD_2Cl_2.

relative to the analogous palladium species are likely due to the stronger chelation to the more oxophilic nickel center.

Reaction of Chelates with Acetonitrile and Ethylene. The reactions of [(N∧N)Pd(κ^2- CH(OAc)Et)][SbF_6] (**4b**) with monodentate ligands were investigated to probe the viability of forming open chelates of the type [(N∧N)Pd(κ^1-CH(OAc)Et)L][SbF_6]. When a sample of **4b** was dissolved in CD_3CN at room temperature and the solution cooled to −30 °C, three products were observed, the dominant of which (ca. 93%) displayed broad resonances for the xylyl and acenaphthyl signals and a broad doublet at 4.35 ppm for the proton α to acetate. The diastereotopic methylene protons β to acetate appear as complex multiplets at 1.2 and 1.5 ppm, while the terminal methyl group γ to acetate appears as a triplet at 0.72 ppm. This species, [(N∧N)Pd(κ^1-CH(OAc)Et)(NCMe)][SbF_6] (**14**$_\alpha$, Scheme 6), was also generated by addition of acetonitrile to **4b** in dichloromethane-d_2 at −78 °C. ^{1}H COSY data allowed the assignment of the other two products which result from migration of palladium along the carbon chain by β-hydride elimination followed by reinsertion: [(N∧N)Pd(κ^1-CH(Me)(CH_2OAc))(NCMe)][SbF_6] (**14**$_\beta$) and [(N∧N)Pd((CH_2)$_3$OAc)(NCMe)][SbF_6] ((**14**$_\gamma$) Scheme 6). Addition of carbon monoxide to this solution at room temperature results in the formation of the three related carbon monoxide insertion products, [(N∧N)Pd(κ^1-C(O)CH(OAc)Et)(NCMe)][SbF_6] (**15**$_\alpha$), [(N∧N)Pd(κ^1-C(O)CH(Me)(CH_2OAc))(NCMe)][SbF_6] (**15**$_\beta$), and [(N∧N)Pd(κ^1-C(O)(CH_2)$_3$OAc)(NCMe)][SbF_6] (**15**$_\gamma$, Scheme 6).

Equilibrium Studies of Ligand Binding to [(N∧N)Pd(CH(OAc)(Et))] (4b). By variation of the temperature (−110 to −70 °C) of solutions of **4b** and acetonitrile in CD_2Cl_2, the temperature dependence of the equilibrium binding constant, K_{eq}, was examined. From these data and the use of the Van 't Hoff equation, values of $\Delta H = -2.1(2)$ kcal/mol and $\Delta S = -9(1)$ eu were obtained for the binding of acetonitrile (Scheme 7).

In a similar manner, methylene chloride solutions of **4b** were charged with varying concentrations of ethylene,[15] and the temperature was varied from −105 to −70 °C. By measurement of the equilibrium between **4b** and the ethylene adduct **16**, values of $\Delta H = -4.1(2)$ kcal/mol and $\Delta S = -23(1)$ eu were obtained for the binding of ethylene.[16]

The ^{1}H NMR spectrum of **16** at −40 °C is similar to that of **14**$_\alpha$, the product which results from reaction with acetonitrile, but the resonances are broader. The methine signal of the carbon chain appears at 4.12 ppm, one of the two diastereotopic methylene signals appears at 1.63 ppm, and the methyl group at 0.33 ppm. The other methylene proton is obscured. The bound

(14) McCord, E. F.; McLain, S. J.; Nelson, L. T. J.; Arthur, S. D.; Coughlin E. B.; Ittel, S. D.; Johnson, L. K.; Tempel, D.; Killian, C. M.; Brookhart, M. *Macromolecules* **2001**, *34*, 362.

(15) Because ethylene distribution between the headspace and solution varied with temperature, ethylene concentration at a given temperature was determined by NMR integration.

(16) Values given for 1 M C_2H_4 as the standard state. It is surprising that such a large difference is observed for the ΔS of acetonitrile vs ethylene binding (−9 eu vs −23 eu). Several factors could conceivably come into play here. Since acetonitrile binds in a linear fashion it loses fewer degrees of freedom upon binding than ethylene which binds in an eta-2 fashion. In addition, ethylene may more extensively restrict the motion of the CH(Et)OAc moiety than CH_3CN would. Unbound CH_3CN may organize the solvent more extensively than free ethylene.

Scheme 7. Van't Hoff Studies of Ethylene and Acetonitrile

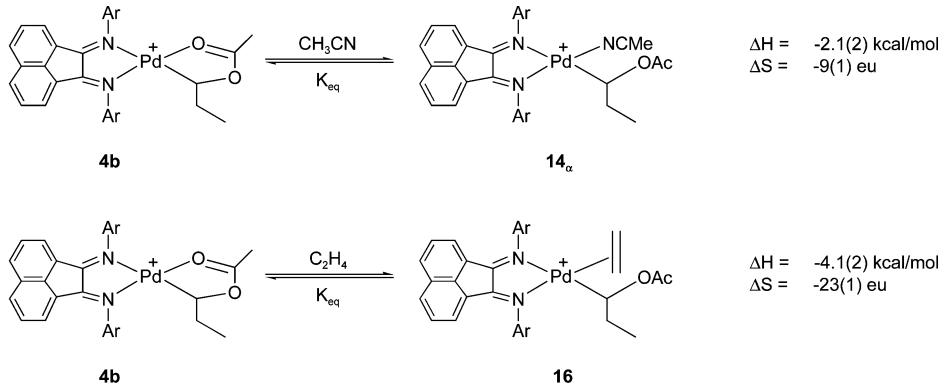

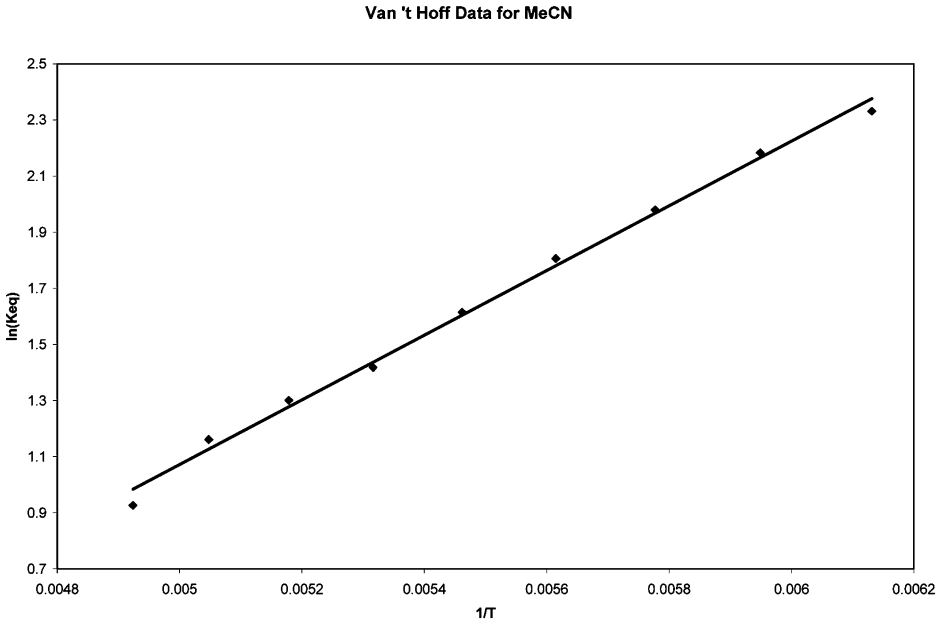

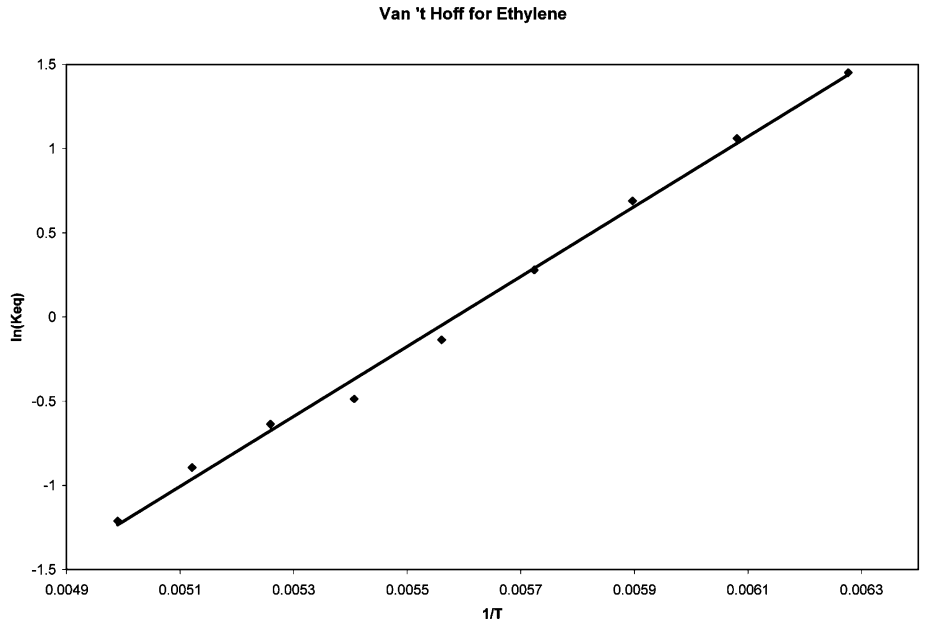

ethylene protons appear as very broad signals at 4.2, 4.3, and two overlapping signals at 4.9 ppm.

The trifluoroacetate chelate [(N∧N)Pd(κ^2-CH(OAc$_f$)(Et)][SbF$_6$] (**6**) is much more easily opened. Addition of even small

Scheme 8. Reactions of Trifluoroacetate Chelate (**6**) with Acetonitrile and Ethylene

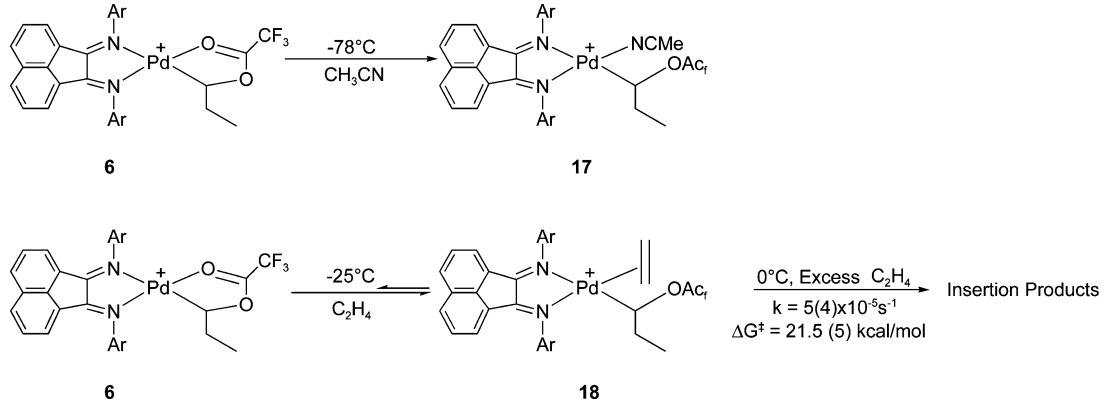

Scheme 9. Relative Binding of Olefins to Palladium Diimine Complexes

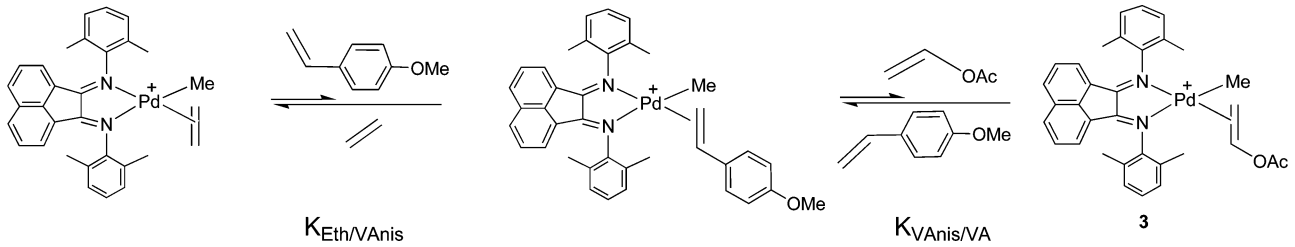

amounts (6.5 equiv, 200 mM) of acetonitrile at −78 °C results in quantitative formation of the open species [(N∧N)Pd(κ^1-CH(OAc$_f$)(Et))(NCMe)][SbF$_6$] (**17**) (Scheme 8).

The ethylene adduct [(N∧N)Pd(κ^1-CH(OAc$_f$)(Et))(C$_2$H$_4$)][SbF$_6$] (**18**) is formed in the presence of 2 equiv of ethylene at −25 °C. Both complexes have NMR spectra much like their acetate analogues, **14a** and **16**, with the protons α to trifluoroacetate appearing at 4.07 and 4.28 for **17** and **18**, respectively. At −40 °C, both NMR spectra are sharp, with the ethylene signal for **18** forming a distinctive AA′BB′ pattern at 4.71 ppm.

The ethylene complex **18** is remarkably stable at −25 °C. At 0 °C, the complex very slowly begins to insert ethylene ($k \approx 5(4) \times 10^{-5}$ s^{-1}, $\Delta G^{\ddagger} = 21.5(5)$ kcal/mol from initial rates) and the growing chain is observable in the ^{1}H NMR spectrum. The measured insertion rate of **18** is approximate, since the first insertion ("initiation") is so much slower than subsequent insertions. Once a small percentage of the palladium centers has been so activated, they consume ethylene very rapidly relative to the disappearance of the starting material, **18**. Maintaining an adequate supply of ethylene in the sample becomes impractical after very early reaction times, and measurement of its rate of disappearance is difficult. However, this very discrepancy in rates in a complex in which the chelate is easily opened clearly demonstrates the inhibitory effect of the OAc$_f$ group on insertion.[17]

Polymerization Studies. As reported previously,[4] MA reacts with the catalyst precursor [(N∧N)PdMe(NCAr$_f$)][B(Ar$_f$)$_4$] (**1**) to form the isolable complex [(N∧N)Pd(κ^2-CH$_2$)$_3$CO$_2$Me][B(Ar$_f$)$_4$] (**19**). This species can be used as a stable, easily handled precursor for the polymerization of ethylene or for the copolymerization of ethylene and MA. Given the similarities between the chelate formed by MA and that formed with vinyl acetate, we have attempted to use the latter complex [(N∧N)Pd(κ^2-CH(OAc)Et)][B(Ar$_f$)$_4$] (**4a**) as such a catalyst precursor. However, at 25 °C and 200 psig of ethylene, over the course of ca. 12 h, 11 μmol of catalyst produced only 81 mg of polyethylene and the polyethylene showed no sign of comonomer incorporation. When **4a** was exposed to ethylene in an NMR tube, slow consumption of ethylene was observed, but no detectable decrease in the concentration of **4a** took place, suggesting that all catalytic activity proceeded from a tiny mole fraction of the catalyst and thus that initiation is far slower than propagation. Since the chelate formed from insertion of VA$_f$, [(N∧N)Pd(OAc$_f$)Et)] (**6**), is more easily opened by ethylene, we also attempted copolymerization reactions of ethylene (400 psig) and VA$_f$ (0.43 M, 5 vol %) using [(N∧N)PdMe(NCAr$_f$)][B(Ar$_f$)$_4$] (**1**) as a precursor in dichloromethane at room temperature. While an appreciable amount of polyethylene was produced (11.4 g polyethylene from 0.1 mmol catalyst), it contained no detectable trifluoroacetate functionalities.

Relative Binding Studies of Olefins. In this and previous studies[3,4] we have demonstrated that olefin binding and exchange are rapid relative to insertion, and thus the copolymerizations are governed by the Curtin−Hammett principle: the relative incorporation of two olefins (A,B) into the polymer is equal to $K_{A/B}k_A/k_B$, where $K_{A/B}$ is the ratio of binding constants of A and B, while k_A and k_B are the two olefin insertion rates. Generation of the palladium olefin complexes at low temperature in situ from (N∧N)PdMeI, AgSbF$_6$, and olefin allows the measurement of the relative binding affinities of two olefins, L and L′ (Scheme 9). While the relative binding constants of ethylene and VA are too different to measure directly, pairwise equilibrium studies with ethylene and *p*-vinyl anisole as well as *p*-vinyl anisole and VA allowed us to determine an equilibrium constant $K_{VA/Eth} = K_{VA/VAnis}K_{VAnis/Eth} = (0.078)(0.011) = (8.6 \times 10^{-4})$ at −95 °C (Table 2). This corresponds to a $\Delta G°$ of 2.5 kcal/mol and a $K_{VA/Eth}$ of 0.015 at 25 °C (assuming a $\Delta S°$ of ca. 0). A similar procedure determined a relative binding constant between VA and VA$_f$ of $K_{VAf/VA} =$ ca. 4.9×10^{-3} at −30 °C and hence a $\Delta G°$ of 2.6 kcal/mol. Thus the overall $\Delta G°$ between ethylene and VA$_f$ is 5.1 kcal/mol, corresponding to a $K_{VAf/Eth} = 1.8 \times 10^{-4}$ at 25 °C.

Table 2. Structural Parameters for the X-ray Diffraction Crystal Structure of [(N∧N)Pd(CH(Et)(OAc))][SbF_6] (**4b**)

parameter	**4b**
empirical formula	$C_{35}H_{37}Cl_4F_6N_2O_2PdSb$
formula weight	1001.63
temperature	173.1 K
wavelength	0.710 73 Å
crystal system, space group	triclinic, $P\bar{1}$ (No. 2)
unit cell dimensions	$a = 8.8149(9)$ Å
	$b = 12.7183(13)$ Å
	$c = 18.3693(19)$ Å
	$\alpha = 91.953(2)°$
	$\beta = 90.798(2)°$
	$\gamma = 108.682(2)°$
volume	1949.1 Å^3
Z, calculated density	2, 1.707 Mg/m^3
absorption coefficient	1.49 mm^{-1} using SADABS
F (000)	990.60
crystal size	0.25 × 0.25 × 0.20 mm^3
index ranges	$-10 \le h \le 9$
	$0 \le k \le 15$
	$-21 \le l \le 21$
reflections collected/unique/ with Inet > 3.0 σ (Inet)	18479/6826/5499
merging *R* value on intensities	0.034
cell dimensions determined by	4274 reflections, $5 \le 2\theta \le 50$
refinement method	full refinement on F_o
residuals (significant reflections)	5435, $R_f = 0.057$, R_w 0.076
residuals (all reflections)	6826, $R_f = 0.073$, R_w 0.084
residuals (included reflections)	5435, $R_f = 0.057$, R_w 0.076, GoF 2.5632
maximum shift/σ ratio	0.008
minimum density of last D-map	−1.550e/Å^3
maximum density of last D-map	1.920e/Å^3
secondary extinction coefficient	0.6221 microns ($\sigma = 0.0801$)

Discussion

There are five fundamental features of these reactions that determine the feasibility of copolymerization of a comonomer with ethylene:

(1) the relative binding strengths of ethylene and the comonomer;

(2) the relative insertion rates of ethylene and the comonomer;

(3) if the inserted comonomer forms a chelate, the ease with which this chelate can be opened to promote subsequent insertions;

(4) the rate of subsequent ethylene insertion into the metal carbon bond following comonomer insertion;

(5) the competition of decomposition with chain propagation.

Features 1 and 2: Relative Binding Constants and Insertion Barriers. We have determined the relative binding constants of VA and ethylene to be 8.6×10^{-4} at −95 °C (Table 2). This ratio corresponds to a $\Delta G°$ of 2.5 kcal/mol and a $K_{VA/Eth}$ of 0.015 at 25 °C assuming that ΔG is temperature independent. For palladium complexes containing this ligand, an Eyring analysis has not been carried out for ethylene insertion, but assuming a similar $\Delta S^‡$ to that for VA complex **8c** (3(5) eu) and using the measured $\Delta G^‡$ at −20 °C (18.4 kcal/mol), a $\Delta G^‡$ of ca. 18.3 kcal/mol can be estimated for ethylene insertion at 25 °C, while that for VA is ca. 19.3 kcal/mol. The estimated difference between the two insertion barriers at 25 °C is therefore ca. 1.0 kcal/mol, corresponding to a rate ratio k_{VA}/k_{Eth} of ca. 0.3. Under equal concentrations of ethylene and VA, and assuming relative binding affinities of 0.015 (see above), this would result in a degree of incorporation of roughly 0.5%. While this is a low percentage, it does imply that, barring other problems, some VA could be incorporated using this palladium catalyst, particularly if high VA/ethylene ratios were employed.

While we have not carried out a full Eyring study of VA_f insertion, the $\Delta G^‡$ at −40 °C was determined to be 17.4(1) kcal/mol ($k_{obs} = 2.43(1) \times 10^{-4} s^{-1}$). The barrier for ethylene insertion at this temperature is estimated to be 18.4 kcal/mol, corresponding to a $\Delta\Delta G^‡$ of 1.0 kcal/mol. The binding energy of VA_f is ca. 5.1 kcal less than that of ethylene at −30 °C. Assuming the differences in these values are temperature independent, and using the same procedure as above for VA, one can predict a degree of incorporation of VA_f of ca. 0.1% at equal ethylene and VA_f concentrations at 25 °C. This extremely low level of expected incorporation probably explains the observation that ethylene, in the presence of VA_f, is polymerized at a rate comparable to the system in the absence of ethylene: VA_f is virtually never incorporated due to its extremely unfavorable binding affinity and thus will have little or no effect on the polymerization. It should be stressed that because these incorporation estimates rely on the assumption that ΔS of binding and $\Delta S^‡$ of insertion are roughly the same for all three olefins, these percentages should be considered approximate.

The rate of VA insertion into the Pd−Me bond of **2** is surprisingly slow ($\Delta G^‡ = 19.3$ kcal/mol at 25 °C for VA) relative to ethylene ($\Delta G^‡ = 18.3$ kcal/mol, 25 °C). The general trend which has been observed for nickel and palladium complexes has been that electron-withdrawing groups, such as acetate ($\sigma_p = 0.31$), accelerate insertion;[4,6a,18,19] however, in this case, vinyl acetate inserts more slowly than ethylene. Hammett studies have been carried out using *para*-substituted styrenes with both early[20] and late[18] transition metals, which have shown that for 2,1 insertion[21] there is an excellent correlation between σ_p and the $\Delta G^‡$ values for insertion, with lower barriers for more electron-withdrawing substituents. Svensson et al. have calculated the insertion barriers for a variety of α-substituted olefins.[22] These calculations suggested that while, in general, more electron-rich olefins inserted more slowly, it was far from an ideal correlation. This is perhaps unsurprising, since an α-substituted olefin is analogous to an *o*-substituted arene, for which Hammett correlations are notoriously problematic for steric reasons. Our results also suggest that great caution should be exercised in drawing such correlations, especially in cases where data sets are very limited.[6a]

Features 3−4: Chelate Opening and Subsequent Insertion. Three possible reasons why VA blocks olefin polymerization are shown in Scheme 10. The first is an unfavorable equilibrium in the opening of the chelate **4** with ethylene (K_{eq}),

(17) It cannot be determined whether species **18** undergoes insertion or if insertion occurs from a species generated by metal migration down the chain which moves the OAc_f group to a the beta or gamma position and generates a species with a much lower barrier to insertion. From observations summarized in Scheme 6, this method for insertion from **18** appears feasible, but the beta and gamma species are clearly higher in energy and the overall effect would still be a much higher apparent barrier of **18**.

(18) Rix, F.; Brookhart, M.; White, P. S. *J. Am. Chem. Soc.* **1996**, *118*, 2436.
(19) Hansch, C.; Leo, A.; Taft, R. W. *Chem. Rev.* **1991**, *91*, 165.
(20) Burger, B. J.; Santarsiero, B. D.; Trimmer, M. S.; Bercaw, J. E. *J. Am. Chem. Soc.* **1988**, *110*, 3134.
(21) The *exo*-insertion of *p*-substituted styrenes reported in ref 20 for Cp_2Nb-(H)(styrene) complexes is analogous to 2,1 insertion and rates are accelerated by electron-withdrawing groups. *Endo*-insertion, corresponding to 1,2 insertion, showed an opposite trend. In other studies by Halpern and Okamato (using rhodium),[23] Bercaw and Doherty (niobium),[24] and Wolczanski and Strazisar (tantalum),[25] more electron *rich* olefins inserted more rapidly. In the first and third cases, the overall rates measured were a combination of both a binding constant and an insertion rate.
(22) von Schenk, H.; Strömberg, S.; Zetterberg, K.; Ludwig, M.; Åkermark, B.; Svensson, M. *Organometallics* **2001**, *20*, 2813.

Scheme 10. Opening the Chelate with and Subsequent Insertion of Ethylene

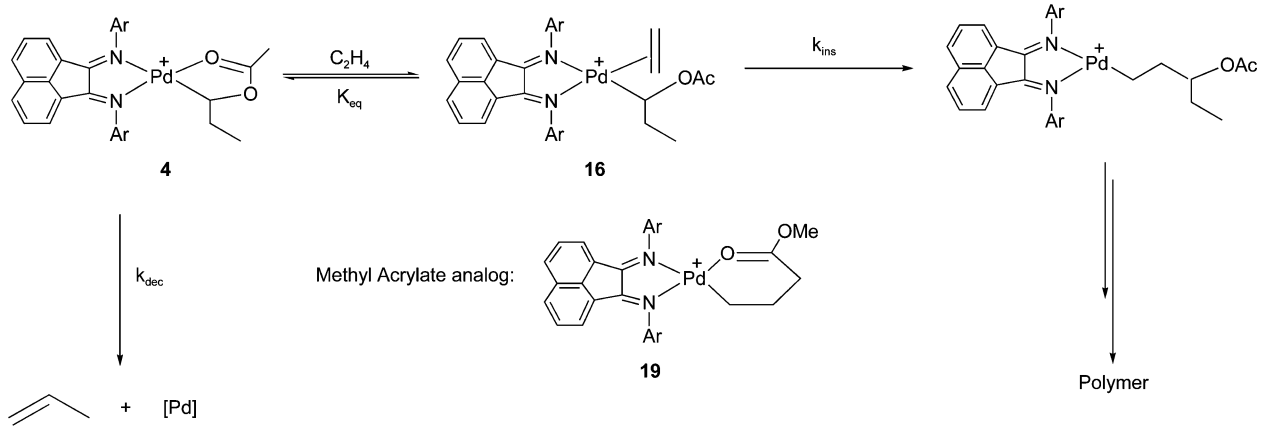

Scheme 11. Comparison of VA and MA Chelates

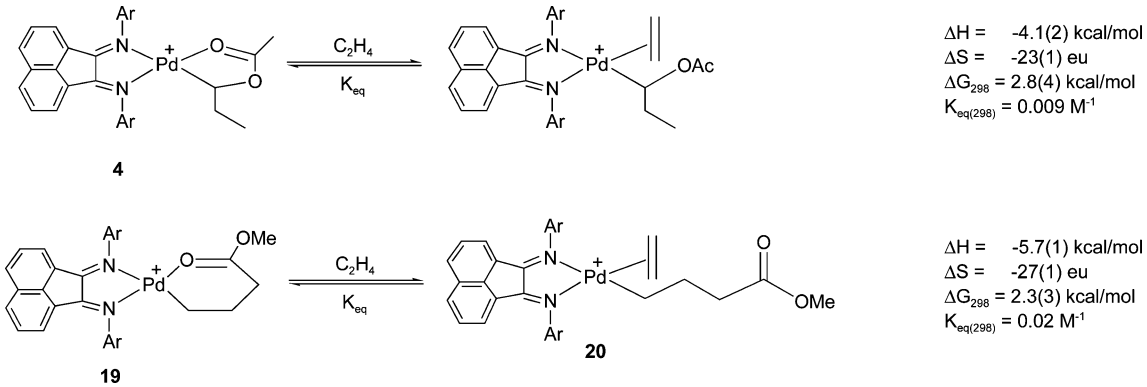

the second is a slow rate of insertion of ethylene into the Pd−C bond of **16** (k_{ins}), and the third is a decomposition pathway (k_{dec}). Since insertion of MA forms a similar chelate species (**19**, also shown) without shutting down catalysis, comparison between the chelate complexes generated by VA and MA is germane to the discussion.

The ease of chelate opening by ethylene can be examined by measuring the equilibrium reaction of **4b** with ethylene over a range of temperatures. As described above, values of $\Delta H = -4.1(2)$ kcal/mol and $\Delta S = -23(1)$ eu were obtained for the reaction of **4** with ethylene, while thermodynamic values of $\Delta H = -5.7(1)$ kcal/mol and $\Delta S = -27(1)$ eu have previously been reported for the opening of **19** (Scheme 11).[4,26]

The calculations performed by Goddard et al. predict ΔE values for these reactions of −1.9 kcal/mol and −3.0 kcal/mol for model complexes of **4** and **19** (the correct relative stabilities), and the $\Delta\Delta E$ of 1.1 kcal/mol agrees reasonably well with the experimental value of $\Delta\Delta H = 1.6(2)$ kcal/mol. Comparison of the ΔG values for the two systems at 25 °C shows that opening of **4** is unfavorable ($K_{eq} = 0.009$ M^{-1}) but not much less favorable than opening of the chelate formed from methyl acrylate ($K_{eq} = 0.02$ M^{-1}), since the difference in $\Delta\Delta S$ partially offsets $\Delta\Delta H$.

A second feature which strongly disfavors propagation in the VA case relative to MA is the rate of subsequent insertion from the open chelate. In the case of MA, the open chelate **20** undergoes insertion with a barrier equal to that of insertion into a normal alkyl group, $\Delta G^{\ddagger} = 18.6$ kcal/mol (see Scheme 12). In contrast, complex **16** bearing an alpha acetoxy group has a much higher barrier to insertion. Unfortunately we have been unable to measure this specific barrier, but based on the results of the VA_f study, a barrier of at least 21.5 kcal/mol can be estimated. This value is in line with calculations by Goddard et al. that have predicted a $\Delta E^{\ddagger}$ of 25.1 kcal/mol for this insertion barrier.[4]

Thus, the barrier for ethylene insertion into the Pd−C bond is approximately 3 kcal/mol greater in the case of **18** than **20**. This is perhaps unsurprising given that the α-carbon of **18** bears a strongly electron-withdrawing substituent, while that of **20** does not. The same holds true of the acetate analogue, **16**. It is well-known that, in alkyl carbonyl complexes, the more electronegative carbon fragments have a lower migratory aptitude.[27] Such behavior has also been predicted by theoretical studies, which have linked this trend to the relative amounts of s- and p-character in the metal−carbon bond of the migrating group.[28] Jordan et al. have recently reported similar behavior with early transition metal olefin insertion processes.[29]

(23) Halpern, J.; Okamoto, T. *Inorg. Chim. Acta* **1984**, *89*, L53.
(24) Doherty, N. M.; Bercaw, J. E. *J. Am. Chem. Soc.* **1985**, *107*, 2670.
(25) Strazisar, S. A.; Wolczanski, P. T. *J. Am. Chem. Soc.* **2001**, *123*, 4728
(26) It should be noted that **19** contains 2,6-diisopropylphenyl groups on the diimine, while the diimine aryls of **4** are 2,6-dimethylphenyl. Typically, differences between rates and equilibria of palladium complexes of varying diimine ligands are small, being on the order of a kcal/mol or less.
(27) (a) Collman, J. P.; Hegedus, L. S.; Norton, J. R.; Finke, R. G. *Principles and Applications of Organotransition Metal Chemistry*; University Science Books: Mill Valley, CA, 1987; pp 370−1. (b) Alexander, J. J. In *The Chemistry of the Metal Carbon Bond*; Hartley, F. R., Ed.; Wiley: New York, 1984; Vol 2, p 259, Table 1. (c) Cotton, J. D.; Crisp, G. T.; Daly, V. A. *Inorg. Chim. Acta* **1981**, *47*, 165. (d) Cotton, J. D.; Crisp, G. T.; Latif, L. *Inorg. Chim. Acta* **1981**, *47*, 171. (e) Cotton, J. D.; Dunstan, P. R. *Inorg. Chim. Acta* **1984**, *88*, 223.
(28) Axe, F. U.; Marynick, D. S. *J. Am. Chem. Soc.* **1988**, *110*, 3728.
(29) Stockland, R. A.; Foley, S. R.; Jordan, R. F. *J. Am. Chem. Soc.* **2003**, *125*, 796.

Scheme 12. Insertion of Ethylene into Various Palladium−Carbon Bonds

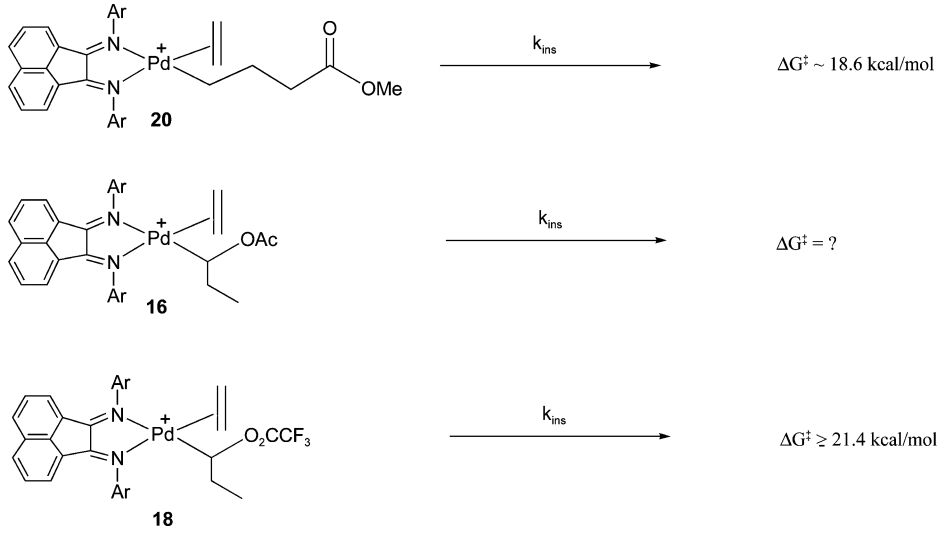

Scheme 13. A High-Energy Decomposition Pathway for $\mathbf{11}_{(1,2)}$

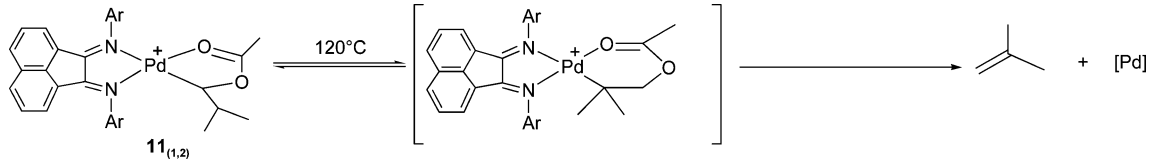

In the case of copolymerization of ethylene and MA, chelate formation substantially retards the rate of chain growth relative to ethylene homopolymerization, and this effect can be attributed solely to an unfavorable equilibrium between the chelate and the ethylene adduct necessary for chain growth. In the case of VA, chelate opening by ethylene is slightly less favorable, and in addition, the subsequent insertion barrier is ca. 3 kcal/mol greater, implying that VA may retard the polymerization rate (relative to ethylene homopolymerization) by another factor of ca. 100. This large rate reduction may well be responsible for nearly complete deactivation of the catalyst by VA.

Feature 5: Catalyst Stability. Catalyst instability may play a role in deactivation by VA and therefore the decomposition of the chelates **4** and **11**−**13** was examined (Table 1). The mechanism of decomposition most likely involves β-hydride elimination and reinsertion, which places the palladium center β to the carboxylate moiety (Scheme 5), allowing a formal β-carboxylate elimination reaction to occur. Such a pathway is well-established by literature precedent[30] and has also been predicted by Goddard and co-workers utilizing DFT calculations.[9] The difference between the decomposition barrier for the *i*Pr-substituted chelate $\mathbf{11}_{(1,2)}$ (Table 1, above) and that of the other chelates is striking. As shown in Scheme 13, rearrangement in this complex to place palladium β to acetate situates the palladium at a sterically hindered tertiary carbon center, thereby accounting for the fact that this intermediate is formed much more slowly than in the other complexes.

As noted above, when vinyl acetate inserts into the Ni−Me bond, both 2,1 and 1,2 insertion products are observed. The 1,2 insertion forms a six-membered chelate analogous to the proposed intermediate in the palladium thermolysis mechanism. This species is considerably less stable than the five-membered 2,1 insertion product, decomposing at −30° rather than 60 °C (Scheme 5). This observation strongly suggests a β rather than α elimination mechanism.

Does the VA chelate in the presence of ethylene decompose competitively with ethylene insertion? Our data cannot answer this question definitively. The barrier for ethylene insertion in opened chelate **16** is almost certainly lower (21−22 kcal/mol) than the barrier to decomposition of chelate **4** (25.5 kcal/mol). However, under low ethylene pressures the equilibrium lies strongly in favor of **4**, which may result in β-acetate elimination competitive with chelate opening and insertion. At high ethylene pressures, the equilibrium can be shifted in favor of open **16**, but the rate of decomposition of **16** via β-acetate elimination is unknown.

Conclusions

These studies establish quantitative aspects of the reactions of vinyl acetate(VA) and vinyl trifluoroacetate (VA_f) with $[(N\wedge N)M(CH_3)]^+$ (M = Pd, Ni, N∧N = *N*,*N*′-1,2-acenaphthylenediylidene bis(2,6-dimethyl aniline) and subsequent reactions with ethylene following insertion of these monomers. Major conclusions from these studies, cast in qualitative terms, can be summarized as follows:

(1) Binding affinity studies show that, relative to ethylene, VA binds weakly and VA_f binds exceedingly weakly to the $[(N\wedge N)PdCH_3]^+$ moiety.

(2) VA and VA_f insertion into the M−CH_3 bond of $[(N\wedge N)MCH_3]^+$ results in the formation of chelate complexes. For Pd, insertion occurs in a 2,1 fashion and yields a five-membered chelate in which the acetoxy group resides at C_α. For Ni, insertion occurs in both a 2,1 and 1,2 fashion to give a mixture of five- and six-membered ring chelates.

(3) Thermolysis of the Pd chelates results in β-acetate and β-trifluoroacetate elimination. Trifluoroacetate eliminates at a rate considerably greater than that of acetate. The five-membered Ni acetate chelate is quite stable at room temperature, while the six-membered chelate from 1,2 insertion of vinyl acetate eliminates readily at −35 °C.

(4) The five-membered chelate formed from VA_f insertion is readily opened by ethylene to form the ethylene adduct $[(N\wedge N)Pd(\kappa^1\text{-}CH(Et)OAc_f)(C_2H_4)]^+$. In the case of the chelate from VA insertion, the equilibrium strongly favors the chelate over the open form $[(N\wedge N)Pd(\kappa^1\text{-}CH(Et)OAc)(C_2H_4)]^+$.

(5) The insertion barrier of ethylene in the opened form of the VA and VA_f chelates is significantly higher (ca. 3 kcal/mol) than the barrier of insertion into a simple $[(N\wedge N)Pd(alkyl)]^+$ bond due to the presence of the electron-withdrawing acetoxy (or trifluoroacetoxy) group at C_α. The rate ratio is estimated to be ca. 1:100 at 25 °C.

(6) Homopolyethylene is generated at good rates when copolymerization of ethylene and VA_f is attempted. This arises simply because VA_f is not incorporated due to the very weak binding of VA_f to the Pd center. VA efficiently quenches catalyst activity in attempts to copolymerize VA and ethylene. This is likely due to incorporation of VA to form the chelate which, due to thermodynamically unfavorable opening with ethylene and a high barrier to insertion of the low equilibrium concentration of the opened form, greatly retards chain propagation. Some catalyst decay through β-acetate elimination cannot be ruled out.

These studies reveal the pitfalls of copolymerization of VA with ethylene and point to the need to redesign catalysts if such copolymerizations are to be successful.

Experimental Section

General Considerations. All manipulations of air and/or water sensitive materials were performed under an argon atmosphere using standard Schlenk or glovebox techniques. Argon was dried by passage through columns of BASF catalyst (Chemalog) and 4 Å molecular sieves. Complexes **4** and **6**−**11** were stored in the glovebox freezer at −30° to −35 °C, as was $[H(OEt_2)_2][B(Ar_f)_4]$. NMR spectra were obtained using Bruker DRX400 and DRX500 spectrometers. NMR probe temperatures were obtained by use of a calibrated Omega type T thermocouple immersed in a 5 mm NMR tube containing anhydrous methanol and calibrated with baths of known temperatures. Elemental analyses were performed by Atlantic Microlab, Inc., Norcross GA. Values for $\Delta G^\ddagger$, $\Delta H^\ddagger$, and $\Delta S^\ddagger$ were obtained from first-order reaction rate data and the Eyring equation. Values for ΔG, ΔH, and ΔS were obtained from equilibrium constant measurements and the Van 't Hoff equation. All error estimates were calculated by standard regression and error propagation techniques. Signals for the $B(Ar_f)_4^-$ counterion are not provided below, as they are invariant from complex to complex and have been previously reported.[2]

Materials. All solvents were deoxygenated and dried via passage through a column of activated alumina.[31] Dichlorofluoromethane-*d* was prepared following the procedure of Siegel and Anet[32] and was distilled at ambient temperature and pressure to remove traces of chloroform-*d*, though it remained a mixture of $CDCl_2F$ and $CDClF_2$. Dichloromethane-d_2 and 1,1,2,2-tetrachloroethane-d_2 were dried over P_2O_5. The α-diimine ligands[33] (COD)PdMeCl,[34] (COD)$PdMe_2$,[35] $(N\wedge N)PdMeCl$,[4] $[(N\wedge N)Pd(OEt_2)][B(Ar_f)_4]$,[2] $[(N\wedge N)NiMe(OEt_2)][B(Ar_f)_4]$,[36] and $[H(OEt_2)_2][B(Ar_f)_4]$[37] were prepared according to literature methods. All other reagents unless otherwise noted were purchased from commercial sources and used without further purification. *n*-Butyl isocyanide, vinyl acetate, and VA_f were vacuum transferred prior to use and dried over 4 Å sieves.

Kinetic Experiments. Kinetics were performed in all cases in an NMR probe on a DRX 500 spectrometer maintained at the temperature in question. Reactions were monitored unless otherwise noted by integration of a peak of the starting material. A delay of 30 s was used between pulses for reactions with half-lives greater than 30 min, 10 s for faster reactions. Reactions were generally followed for 2.5−3.5 half-lives, with the exception of the two lowest temperatures in the Eyring study, which were monitored for 0.8 and 0.6 half-lives. Low-temperature experiments were performed in an oven-dried NMR tube which was charged with solid reagents in a glovebox and capped with a septum. Subsequently, the tube was cooled in a −78 °C bath, and solvent and liquid reagents were added slowly via syringe. High-temperature experiments were carried out in a J. Young tube, charged with solids and solvent in the drybox.

Preparation of (N∧N)PdMeI. A Schlenk flask was charged with (N∧N)PdMeCl (169.2 mg, 0.310 mmol) and sodium iodide (53.6 mg, 0.358 mmol) in the drybox. Dichloromethane (12 mL) and acetone (15 mL) were added, and the reaction was allowed to stir for several minutes. The solvent was removed under vacuum, and the solids were taken up in dry methylene chloride (15 mL) and cannula filtered into a flame-dried Schlenk flask. The volume was reduced to 5 mL under vacuum, and methanol (15 mL) was added, with concomitant formation of precipitate. The solvent was removed under reduced pressure to give an iridescent, burgundy crystalline material (158 mg, 80% yield). ^{1}H NMR (400 MHz $CDCl_3$): 8.11, 8.06 (both d, 8 Hz, 1H each, H3 and H8 of acenaphthyl group), 7.49 (apparent q, 2H, H4 and H7 of acenaphthyl group), 7.2−7.3 (m, 6H, N−Aryl protons), 6.75, 6.64 (both d, 8 Hz, 1H each, H4 and H4 of acenaphthyl group), 2.33, 2.33 (6H each, N−Ar methyl groups), 0.67 (3H, Pd−Me). ^{1}H NMR ($CDCl_3$): δ = 0.60 (s, 3H, Pd−**Me**), 2.28, 2.29 (s, 12H total, Ar−**Me**), 6.57, 6.68 (both d, 7.2 Hz, H3 and H8 of acenaphthyl backbone), 7.2−7.3 (6H, m, Ar), 7.45 (2H, m, H4 and H7 of acenaphthyl backbone), 8.05, 8.10 (both d, 8.4 Hz, 1H, H5 and H6 of acenaphthyl backbone). ^{13}C NMR ($CDCl_3$): δ = −3.9 (Pd−**Me**), 18,3, 19.1 (2C each, Ar**Me**), 123.9, 123.9, 126.4, 126.5, 127.3, 127.5, 128.3, 128.8, 128.9, 129.2, 130.8, 131.3, 131.3, 142.8, 144.1, 144.8, 167.7, 171.1. Anal. Calcd For $C_{29}H_{27}IN_2Pd$: C, 54.69; H, 4.27; N, 4.40. Found: C, 54.18; H, 4.26; N, 4.35.

Preparation of $[(N\wedge N)PdMe(OEt_2)][SbF_6]$ (2b). A flame-dried Schlenk flask was charged with (N∧N)PdMeI (198.0 mg, 0.310 mmol) and $AgSbF_6$ (108.1 mg, 0.315 mmol) and cooled to −78 °C. Ether (1 mL) and dichloromethane (10 mL) were added slowly. Immediately, a flocculent precipitate (AgI) formed. The orange solution was separated from the precipitate by cannula filtration at −78 °C. Ether (5 mL) was added, and the solvent was removed in vacuo at −10 °C to form an orange, tacky oil. Ether (10 mL) was added, and the product was scraped from the sides and stirred vigorously for ca. 1 h to form a fine, canary yellow powder. The ether was removed by cannula filtration, and the solid dried under vacuum at −40 °C for ca. 2 h (195.2 mg, 77% yield). ^{1}H NMR (500 MHz, CD_2Cl_2): 8.21, 8.18 (both d, 8.4 Hz, 1H each, H3 and H8 of acenaphthyl group), 7.50 (m, 2H, H4 and H7 of acenaphthyl group), 7.3−7.4 (m, 6H, N−Aryl protons), 6.85, 6.78 (both d, 7.2 Hz, 1H each, H5 and H6 of acenaphthyl group), 3.42 (q, 6.8 Hz, 4H, $CH_3C\mathbf{H_2}O$), 2.33, 2.33 (6H each, N−Ar methyl groups), 1.47 (t, J = 7.0 Hz, 6H, $C\mathbf{H_3}CH_2O$), 0.64 (3H, Pd−Me). ^{13}C NMR (125 MHz, CD_2Cl_2): δ = 9.1 (Pd−**Me**), 16.1 ($\mathbf{C}H_3CH_2O$, 2C), 17.7 (4C, Ar**Me**), 72.1, (2C, $CH_3\mathbf{C}H_2O$), 124.8, 124.9, 125.1, 125.2, 127.1 127.7, 128.4,

(30) (a) Cheng, J. C.-Y.; Daves, G. D., Jr. *Organometallics* **1986**, *5*, 1753. (b) Zhu, G.; Lu X. *Organometallics* **1995**, *14*, 4899. (c) Zhang, Z.; Lu, X.; Xu, Z.; Zhang, Q.; Han, X. *Organometallics* **2001**, *20*, 3724.
(31) Pangborn, A. B.; Giardello, M. A.; Grubbs, R. H.; Rosen, R. K.; Timmers, F. J. *Organometallics* **1996**, *15*, 1518−1520.
(32) Siegel, J. S.; Anet, F. A. L. *J. Org. Chem.* **1988**, *53*, 2629−2630.
(33) van Koten, G.; Vrieze, K. *Adv. Organomet. Chem.* **1982**, *21*, 151−239.
(34) Rülke, R. E.; Ernsting, J. M.; Spek, A. L.; Elsevier, C. J.; van Leeuwen, P. W. N. M.; Vrieze, K. *Inorg. Chem.* **1993**, *32*, 5769.
(35) Prepared from (COD)PdMeCl[34] and MeLi as per the procedure reported for the synthesis of the analogous Pd complex with 2,6-diisopropyl groups attached to the nitrogen ligand in ref 2.
(36) Svejda, S. A.; Johnson, L. K.; Brookhart, M. *J. Am. Chem. Soc.* **1999**, *121*, 10634−10635.
(37) Brookhart, M.; Grant, B.; Volpe, A. F., Jr. *Organometallics* **1992**, *11*, 3920−3922.

128.6, 129.3, 129.3, 129.5, 130.9, 132.4, 133.1, 142.4, 143.5, 145.4, 168.9, 175.0. The complex is insufficiently stable for elemental analysis.

In Situ Generation of [(N∧N)PdMe(η^2-C_2H_3OAc)][SbF_6] (3b). An NMR tube was charged in the glovebox with (N∧N)PdMeI (25.3 mg, 39.7 μmol) and $AgSbF_6$ (13.6 mg, 39.6 μmol) and was capped with a septum. Outside the box, the tube was cooled to −78 °C and CD_2Cl_2 (650 μL) and VA (5 μL, 50 μmol, 1.4 equiv) were slowly added via syringe. The tube was vigorously shaken and centrifuged in short intervals so that the temperature could be kept as low as possible. ^{1}H (400 MHz, CD_2Cl_2, −37 °C): δ 0.46 (s, 3H, Pd-**Me**), 2.16 (s, 3H, O_2C**Me**), 2.22, 2.24, 2.27, 2.39 (all s, 3H each, NAr−**Me**), 4.04, 4.17 (br d, 4 Hz and 12 Hz, 1H each, methylidene protons), 6.65, 6.74 (d, 7.2 Hz each, 1H each, H5 and H6 of acenaphthyl group), 7.2 (br, unresolved from free vinyl acetate, methine proton of vinyl acetate), 7.2−7.40 (m, 6H, N−**Ar**), 7.57 (two overlapping dd, $J \approx 2$ Hz, 5−10 Hz, H4 and H7 of acenaphthyl group), 8.22, 8.25 (d, 8.4 Hz, 8.0 Hz, H3 and H8 of acenaphthyl group). ^{13}C NMR (100 MHz, CD_2Cl_2, −37 °C): δ = 17.1 (br, Pd−CH_3), 17.6, 17.8, 17.9, 17.9 (Ar−CH_3), 20.5 (CO_2**C**H_3), 66.1 (br, methylidene, vinyl acetate moiety), 124.5 (br, methine carbon, vinyl acetate moiety), 124.4, 124.5, 125.2, 126.1, 126.9, 127.1, 128.1, 128.3, 128.4, 128.5, 129.3, 129.3, 129.5, 129.5, 129.5, 129.7, 130.8, 133.0, 133.9, 141.1, 146.3, 171.0, 175.9, 186.7 (C═O). The complex is insufficiently stable for elemental analysis, but converts to **4b** (vide infra).

Preparation of [(N∧N)Pd(κ^2-CH(Et)(OAc))][$B(Ar_f)_4$] (4a). A flame-dried Schlenk flask was charged with [(N∧N)PdMe($NCAr_f$)]-[$B(Ar_f)_4$] (**1a**) (665.7 mg, 0.413 mmol) in the drybox and brought out to the Schlenk line, where it was lowered to 0 °C. Dry dichloromethane (10 mL) and vinyl acetate (85 μL, 0.92 mmol) were added via syringe. The reaction was allowed to stir for ca. 2 h while warming to 20 °C. The product was purified by column chromatography (Et_2O, silica) and crystallization from dichloromethane/pentane at −30 °C. The product was a mustard microcrystalline powder (140 mg, 23% yield). NMR spectra identical to those of **4b** (vide infra) except for peaks attributable to $B(Ar_f)_4^-$. Anal. Calcd for $C_{65}H_{45}BF_{24}N_2O_2Pd$ (**4a**): C, 53.50; H, 3.11; N, 1.92. Found: C, 53.42; H, 3.19; N, 1.96.

Preparation of [(N∧N)Pd(κ^2-CH(Et)(OAc))][SbF_6] (4b). A flame-dried Schlenk flask was charged with (N∧N)PdMeCl (790.8 mg, 1.45 mmol) and $AgSbF_6$ (507.2 mg, 1.48 mmol) in the drybox. Dry dichloromethane (20 mL) and vinyl acetate (2 mL, 22 mmol) were precooled to −78 °C in a second flame-dried Schlenk flask. The dichloromethane was added to the solids by cannula transfer. The reaction was allowed to stir for ca. 1.5 h and was then warmed to −20 °C for another hour. The orange suspension was cannula filtered into a new flame-dried flask to afford a clear orange solution. The solvent was removed in vacuo, and the product was extracted with THF (35 mL) and cannula filtered a second time to remove a yellow insoluble powder. The solvent was reduced to ca. 10 mL under vacuum and layered with 50 mL of ether. The crystallization solution was allowed to stand at −30 °C for a week. An orange solid was isolated (902.1 mg, 75% yield). ^{1}H NMR ($CDCl_3$, 400 MHz): δ = 0.87 (m, 1H, CH_3C**H**H′CH(OAc)Pd), 1.07 (t, 7 Hz, 3H, C**H**$_3$$CH_2$CH(OAc)Pd), 1.15 (m, 1H, CH_3CH**H**′CH(OAc)Pd), 2.22 (s, 3H, CO_2C**H**$_3$), 2.27 (s, 3H, Ar−C**H**$_3$), 2.41 (s, 3H, Ar−C**H**$_3$), 2.44 (s, 3H, Ar−C**H**$_3$), 2.57 (s, 3H, Ar−C**H**$_3$), 5.50 (dd, 2 Hz, 5 Hz, 1H, CH_3CH_2C**H**(OAc)Pd), 6.66, 6.89 (d, 7 Hz each, 1H each, H3 and H8 of acenaphthyl ligand), 7.3−7.5 (m, 6H, N−Ar signals), 7.60, 7.62 (apparent dt, 8.2 Hz, 2H, H4 and H7 of acenaphthyl ligand), 8.23, 8.27 (apparent dd, 8 Hz, 2H, H4 and H5 of acenaphthyl ligand). ^{13}C NMR (CD_2Cl_2, 125 MHz): δ = 12.4 (PdCH(OAc)CH_2**C**H_3), 17.8 (O_2C**C**H_3), 18.4, 18.4, 18.4, 18.5 (Ar-**C**H_3), 29.0 (PdCH(OAc)**C**H_2CH_3), 105.5 (Pd-**C**H), 124.5, 124.7, 125.1, 125.3, 127.7, 127.9, 128.1, 128.6, 128.8, 129.1, 129.1, 129.3, 129.4, 129.5, 129.6, 130.2, 131.3, 133.0, 133.8, 142.3, 143.1, 146.2, 169.5, 175.6 (aryl carbons), 186.6 (**C**═O). Anal. Calcd for $C_{36}H_{43}F_6N_2O_3PdSb$ (**4b**·Et_2**O**, matches NMR integration): C, 48.37; H, 4.85; N, 3.13. Found: C, 48.43; H, 4.47; N, 3.26.

X-ray Crystal Structure of [(N∧N)Pd(κ^2-CH(Et)(OAc))][SbF_6] (4b). X-ray quality crystals of **4b** were grown from slow diffusion of pentane into a solution of methylene chloride, which contained two methylene chloride molecules in the unit cell. A single crystal was mounted on a Bruker SMART 1K diffractometer at −100 °C, using the ω-scan mode. Selected bond lengths and angles are reported in Figure 2 (Results), while structural parameters are given in Table 2. There are two methylene chloride molecules of crystallization.

In Situ Formation of Cationic Nickel Olefin Complexes. A vacuum-dried Wilmad 528-PP screw-cap NMR tube was charged with **7** (13.9 mg, 0.01 mmol) in the drybox and cooled to −80 °C, and CD_2Cl_2 (0.70 mL) was added slowly via gastight syringe. The tube was briefly shaken to dissolve the sample. A solution of vinyl acetate or VA_f in CD_2Cl_2 (0.10 mL of a 0.20 M solution, ca. 2 equiv) was added to the tube at −80 °C, and the tube was transferred to the precooled NMR probe. Displacement of the ether ligand by the acetate moiety and insertion to form the corresponding chelate species were monitored by variable temperature ^{1}H NMR.

[(N∧N)Ni(κ^2-CH(Et)(OAc))][$B(Ar_f)_4$] ($9_{(2,1)}$). This complex was also synthesized on a preparatory scale, by treating a solution of **7** (125 mg, 0.089 mmol) in CH_2Cl_2 at −80 °C under Ar with a solution of vinyl acetate in CH_2Cl_2 (0.9 mL of a 0.20 M solution, 2 equiv). The reaction was allowed to warm slowly to 0 °C and stirred for 1 h. All solvent was removed in vacuo, and the dark purple solid was dried in vacuo for 1 h at rt, recovered in the drybox, and stored at −35 °C. Yield of $\mathbf{9_{(2,1)}}$ = 76 mg (61%).^{1}H NMR (CD_2Cl_2, 500 MHz) δ 8.17 (d, J = 8.5 Hz, 1H, An H_p), 8.14 (d, J = 8.5 Hz, 1H, An $H_{p'}$), 7.70 (s, 8H, BAr_4'), 7.56 (t, J = 7.5 Hz, 1H, An H_m), 7.54 (s, 4H, BAr_4'), 7.49 (t, J = 7.5 Hz, 1H, An $H_{m'}$), 7.40−7.26 (m, 6H, Ar*H*), 6.85 (d, J = 7.0 Hz, 1H, An H_o), 6.55 (d, J = 7.0 Hz, 1H, An $H_{o'}$), 4.92 (dd, J = 5.0, 2.0 Hz, 1H, NiC*H*), 2.70, 2.56, 2.37, 2.23 (s, 3H each, ArCH_3), 1.99 (s, 3H, NiCH(OC(O)CH_3)), 1.34 (m, 1H, NiCH(C*H*H′CH_3)), 1.25 (t, J = 7.0 Hz, 3H, NiCH(CHH′CH_3)), 0.68 (m, 1H, NiCH(CH*H*′CH_3)). ^{13}C{^{1}H} NMR (CD_2Cl_2, 25 °C, 125 MHz) δ 187.8 (O*C*(O)CH_3), 174.9 and 169.4 (N═*C*—*C*═N), 162.1 (q, $^1J_{CB}$ = 49.6 Hz, BAr'_4 C_{ipso}), 147.6, 142.6 and 142.1 (ligand Ar and Ar′ C_{ipso}), 135.2 (BAr'_4 C_o), 133.4, 133.0, 131.8, 130.7, 130.5, 130.0, 129.9, 129.73, 129.70, 129.52, 129.46, 129.42, 129.2 ($^2J_{CF}$ = 28.5 Hz, BAr'_4 C_m), 129.16, 129.0, 128.2, 125.7, 125.5, 125.1, 124.9 ($^1J_{CF}$ = 270.9 Hz, BAr'_4 CF_3), 124.6, 117.8 (BAr'_4 C_p), 28.4 (NiCH(*C*HH′CH_3), 18.7 and 18.5 (Ar *C*H_3 and *C*′H_3), 18.14 (Ar *C*″H_3), 18.11 (Ni*C*H), 17.8 (OC(O)*C*H_3), 17.7 (Ar *C*‴H_3), 12.5 (NiCH(CHH′*C*H_3). Anal. Calcd for $C_{65}H_{45}BN_2O_2F_{24}Ni$: C, 55.31; H, 3.21; N, 1.98. Found: C, 54.19; H, 3.32; N, 1.93.

[(N∧N)Ni(κ^2-$CH_2CH(CH_3)(OC(O)CH_3)$)][BAr_4'] ($9_{(1,2)}$). ^{1}H NMR (CD_2Cl_2, −50 °C, 500 MHz) δ 8.11 (apparent t (overlapping d), 2H, An H_p and $H_{p'}$), 7.70 (s, 8H, BAr_4'), 7.51 (s, 4H, BAr_4'), 7.45 (t, J = 7.5 Hz, 1H, An H_m), 7.33 (t, J = 7.5 Hz, 1H, An $H_{m'}$), 7.31−7.22 (m, 6H, Ar*H*), 6.88 (d, J = 7.5 Hz, 1H, An H_o), 6.37 (d, J = 7.5 Hz, 1H, An $H_{o'}$), 3.57 (br m, 1H, NiCHH′C*H*), 2.42, 2.41, 2.38, 2.26 (s, 3H each, ArCH_3), 1.79 (s, 3H, NiCHH′CH(OC(O)CH_3)), 1.21 (d, 3H, J = 7.0 Hz, 1H, NiCHH′CH(CH_3)), 1.03 (dd, J = 11.0, 3.0 Hz, 1H, NiC*H*H′), 0.82 (dd, J = 11, 5 Hz, 1H, NiCH*H*′). The complex is insufficiently stable for elemental analysis.

[(N∧N)Ni(κ^2-CH(Et)(OAc_f)] [BAr_4'] (10). ^{1}H NMR (CD_2Cl_2, 20 °C, 500 MHz) δ 8.20 (d, J = 8.5 Hz, 1H, An H_p), 8.18 (d, J = 8.5 Hz, 1H, An $H_{p'}$), 7.71 (s, 8H, BAr_4'), 7.59 (t, J = 8.0 Hz, 1H, An H_m), 7.54 (s, 4H, BAr_4'), 7.53 (t, J = 7.5 Hz, 1H, An $H_{m'}$), 7.45−7.23 (m, 6H, Ar*H*), 6.91 (d, J = 7.5 Hz, 1H, An H_o), 6.58 (d, J = 7.0 Hz, 1H, An $H_{o'}$), 5.38 (dd, J = 5.0, 2.5 Hz, 1H, NiC*H*), 2.73, 2.58, 2.39, 2.28 (s, 3H each, ArCH_3), 1.43 (m, 1H, NiCH(C*H*H′CH_3)), 1.31 (t, J = 7.0 Hz, 3H, NiCH(CHH′CH_3)), 0.81 (m, 1H, NiCH(CH*H*′CH_3)). The complex is insufficiently stable for elemental analysis.

In Situ Generation of [(N∧N)PdMe(η^2-$C_2H_3OAc_f$)][SbF_6] (5): A procedure identical to that used for the acetate analogue, **3b** , was used to generate **5**. ^{1}H NMR (400 MHz, CD_2Cl_2, −25 °C): δ 0.47 (s, 3H, Pd-**Me**), 2.22, 2.25, 2.25, 2.37 (all s, 3H each, NAr−**Me**), 4.29, 4.66

(both br, coupling indistinct, 1H each, methylidene protons), 6.63, 6.74 (d, 7.2 Hz each, 1H each, H5 and H6 of acenaphthyl group), 6.9 (br, unresolved from free vinyl trifluoroacetate, methine proton of vinyl trifluroacetate) 7.26−7.46 (m, 6H, N−**Ar**), 7.58 (two overlapping signals, coupling unresolved, H4 and H7 of acenaphthyl group), 8.23, 8.27 (d, 8.4 Hz each, H3 and H8 of acenaphthyl group). The complex is insufficiently stable for elemental analysis but converts to **6** (vide infra).

Preparation of [(N∧N)Pd(κ^2-CH(Et)(O_2CCF_3))][SbF_6] (6). In the glovebox, a flame-dried Schlenk was charged with (N∧N)PdMeCl (227.6 mg, 0.417 mmol) and $AgSbF_6$ (148.8 mg, 0.433 mmol). The flask was brought out to the vacuum line and lowered to −78 °C. Dry CH_2Cl_2 (22 mL) was cooled in a separate flame-dried Schlenk flask and transferred via cannula to the solids. Almost immediately, a yellow, flocculent precipitate was formed. The reaction was allowed to stir for ca. 30 min, and VA_f (100 μL, 0.86 mmol) was added via gastight syringe. The reaction was warmed to −20 °C for 30 min and was then cannula-filtered into another flame-dried Schlenk flask. The resultant orange solution was kept at −20 °C and evaporated to dryness in vacuo, yielding a foamy solid. The product was crystallized from CH_2Cl_2/diethyl ether at −35 °C to afford brownish clumps which were washed with ether at −20 °C (252 mg, 68% yield). ^{1}H NMR (CD_2Cl_2, 500 MHz, 253 K): δ = 1.05 (br. t, 3H, CH(O_2CCF_3)$CH_2C\mathbf{H_3}$); 0.90 and 1.20 (br. m, 1H each, CH(O_2CCF_3)$C\mathbf{H_2}CH_3$); 2.17, 2.28, 2.32, 2.40 (s, 3H each, N−aryl−$C\mathbf{H_3}$); 5.83 (br. d, 1H, 8.4 Hz, $C\mathbf{H}(O_2CCF_3)$(Et)); 6.65 and 6.80 (d, 1H each, 8 Hz, acenaphthyl H3, H8); 7.3 (m, 10H, N−Aryl protons (*m* and *p*) plus *p* protons of $B(Ar_f)_4^-$); 7.6 (br s, 8H, *o* protons of $B(Ar_f)_4^-$); 8.12 (dd, 2H, 8.0 Hz, 7.6 Hz, acenaphthyl H4, H7); 8.15 and 8.18 (d, 1H each, 8.4 Hz, 8.8 Hz, acenaphthyl H5, H6). ^{13}C NMR (CD_2Cl_2, 253 K, 125 MHz): δ = 11.8 (CH(O_2CCF_3)$CH_2\mathbf{C}H_3$); 17.6, 18.1, 18.2, 18.4 (N−Aryl−$\mathbf{C}H_3$); 28.9 (CH(O_2CCF_3)-$\mathbf{C}H_2CH_3$); 114.8 ($\mathbf{C}$H(O_2CCF_3) CH_2CH_3); 124.4, 124.6, 128.3, 129.7, 130.7, 130.8, 133.5, 134.5 (aromatic and acenaphthyl **C**−H carbons); 126.0, 126.2, 128.8, 128.9, 129.2, 129.7, 131.5, 141.9, 142.9, 147.4, 171.0, 177.6 (quaternary aromatic and acenaphthyl carbons). Carbonyl ($O_2\mathbf{C}CF_3$) and trifluoromethyl carbons not found. **6b** was insufficiently stable for elemental analysis.

Preparation of [(N∧N)Pd(κ^2-CH(R)(OAc))] [SbF_6] R = *i*Pr, *n*Pr, ($\mathbf{11}_{(1,2)}$, $\mathbf{11}_{(2,1)}$). A flame-dried Schlenk flask was charged with (N∧N)PdMeCl (370.7 mg, 0.680 mmol) and $AgSbF_6$ (237.2 mg, 0.690 mmol) in the drybox. The flask was brought out to the Schlenk line and cooled in a −78 °C bath. Dry ether (10 mL) was added, followed by dry dichloromethane (10 mL) and allyl acetate (75 μL, 0.695 mmol). The reaction warmed to −25 °C over the course of 1.5 h and then warmed to room temperature with a water bath. The cold bath was removed, and the reaction allowed to warm to room temperature over the course of an hour. The solution was separated from the silver chloride precipitate by cannula filtration. The solvent was removed in vacuo, and the product crystallized from THF/ether at −30 °C. Two crystal forms were noted: red-orange plates (114 mg, 20% yield) and yellow microcrystals (241 mg, 41% yield). These were separated by the method of Pasteur. The red-orange plates were nearly pure [(N∧N)Pd(CH(*n*Pr)(OAc))] [SbF_6] ($\mathbf{11}_{(2,1)}$), while the yellow crystallites were a mixture of the two isomers. ^{1}H NMR of $\mathbf{11}_{(2,1)}$ ($CDCl_3$, 400 MHz): δ = 0.781 (t, 7.2 Hz, 3H, $C\mathbf{H_3}CH_2CH_2$), 1.25 (m, 2H, $CH_3C\mathbf{H_2}CH_2$), 1.69 (m, 2H, $CH_3C\mathbf{H_2}CH_2$), 2.20 (s, $O_2CC\mathbf{H_3}$), 2.28, 2.42, 2.43, 2.59 (all s, 3H ea, Ar−$C\mathbf{H_3}$), 5.53 (dd, 2 Hz, 6 Hz, $C\mathbf{H}$(OAc)(*n*Pr)Pd)), 6.67, 6.89 (both d, 7.2 Hz ea, 1H each, H3 and H8 of acenaphthyl ring), 7.62, 7.58 (both t, each 7.2 Hz, 1H each, H4 and H7 of acenaphthyl ring), 8.23, 8.27 (both d, 8.0, 8.4 Hz, 1H each, H5 and H6 of acenaphthyl ring). ^{1}H NMR of $\mathbf{11}_{(1,2)}$ ($CDCl_3$, 400 MHz, many peaks obscured by $\mathbf{11}_{(2,1)}$): 0.65 (d, 6.4 Hz, 6H, $(C\mathbf{H_3})_2$CHCH-(OAc)Pd), 1.23 (obscured, seen by COSY, $(CH_3)_2C\mathbf{H}$CH(OAc)Pd), 2.19 (s, 3H, $CO_2C\mathbf{H_3}$), 2.20, 2.30, 2.41, 2.47, (all s, 3H each, Ar−$C\mathbf{H_3}$), 5.45 (obscured, seen by COSY, $(CH_3)_2$CHC$\mathbf{H}$(OAc)Pd), 6.66, 6.88 (d, 1H each, 7.4 Hz, 1H each, H3 and H8 of acenaphthyl ring), 7.25−7.55 (obscured by $\mathbf{11}_{(2,1)}$, identified by COSY and HMBC, N−Ar), 7.54 (obscured, seen by COSY, 1H each, H4 and H7 of acenaphthyl ring), 8.1 (obscured, seen by COSY, 2H, H5 and H6 of acenaphthyl ring). Anal. Calcd for $C_{34}H_{35}N_2O_2PdSbF_6$ ($\mathbf{11}_{(2,1)}$): C, 48.28; H, 4.17; N, 3.31. Found: C, 48.59; H, 4.42; N, 3.19. Anal. Calcd for $C_{34}H_{35}N_2O_2PdSbF_6$ ($\mathbf{11}_{(1,2)}$ and $\mathbf{11}_{(2,1)}$): C, 48.28; H, 4.17; N, 3.31. Found: C, 48.68; H, 4.53; N, 3.13.

Preparation of [(N∧N)Pd(κ^2-CH(R)(OAc))] [SbF_6] R = *i*Bu, *n*Bu, ($\mathbf{12}_{(2,1)}$, $\mathbf{12}_{(1,2)}$). A flame-dried Schlenk flask was charged with (N∧N)PdMeCl (220.0 mg, 0.403 mmol) and $AgSbF_6$ (137.7 mg, 0.401 mmol) in the drybox. The flask was brought out to the Schlenk line and cooled in a −78 °C bath. Dry ether (10 mL) was added, followed by dry dichloromethane (12 mL) and 3-butenyl acetate (60 μL, 0.88 mmol). After 1 h, the cold bath was removed, and the reaction was allowed to warm to room temperature over the course of an hour. The solution was separated from the silver chloride precipitate by cannula filtration. The solvent was removed in vacuo, and the product crystallized from THF/ether at −30 °C (orange crystals, 222 mg, 55% yield). ^{1}H NMR ($CDCl_3$, 400 MHz): 0.40 (d, 6.4 Hz, $(C\mathbf{H_3})_2CHCH_2$-CH(OAc)Pd of $\mathbf{12}_{(1,2)}$), 0.84 (t, 7.0 Hz, $C\mathbf{H_3}CH_2CH_2CH_2CH$(OAc)Pd of $\mathbf{12}_{(2,1)}$), 1.1−1.2 (m, $(CH_3)_2C\mathbf{H}CH_2CH$(OAc)Pd of $\mathbf{12}_{(1,2)}$ and $CH_3C\mathbf{H_2}CH_2CH_2CH$(OAc)Pd of $\mathbf{12}_{(2,1)}$), 1.2−1.3 (m, $CH_3CH_2C\mathbf{H_2}CH_2$-CH(OAc)Pd of $\mathbf{12}_{(2,1)}$), 1.6−1.7 (m, $CH_3CH_2CH_2C\mathbf{H_2}CH$(OAc)Pd of $\mathbf{12}_{(2,1)}$ and $(CH_3)_2CHC\mathbf{H_2}CH$(OAc)Pd of $\mathbf{12}_{(1,2)}$), 2.19 (s, $CO_2C\mathbf{H_3}$ of $\mathbf{12}_{(1,2)}$), 2.21 (s, $CO_2C\mathbf{H_3}$ of $\mathbf{12}_{(2,1)}$), 2.28, 2.41, 2.42, 2.56 (N−Ar−$C\mathbf{H_3}$ of $\mathbf{12}_{(1,2)}$), 2.27, 2.41, 2.43, 2.56 (N−Ar−$C\mathbf{H_3}$ of $\mathbf{12}_{(2,1)}$), 5.49 (dd, 2.2 Hz, 6.6 Hz, $CH_3CH_2CH_2CH_2C\mathbf{H}$(OAc)Pd of $\mathbf{12}_{(2,1)}$), 5.54 (br dd, coupling unresolved, $(CH_3)_2CHCH_2C\mathbf{H}$(OAc)Pd of $\mathbf{12}_{(1,2)}$), 6.64, 6.87 (d, 7 Hz each, H3 and H8 of acenaphthyl ring of **9**), 6.66, 6.88 (d, 7 Hz each, H3 and H8 of acenaphthyl ring of $\mathbf{12}_{(2,1)}$), 7.25−7.55 (N−Ar of both $\mathbf{12}_{(1,2)}$and $\mathbf{12}_{(2,1)}$), 7.57−7.67 (m, H4 and H7 of acenaphthyl ring of $\mathbf{12}_{(1,2)}$and $\mathbf{12}_{(2,1)}$, unambiguously assigned by COSY), 8.24, 8.27 (d, 1H each, 8 Hz, H5 and H6 of acenaphthyl ring of $\mathbf{12}_{(2,1)}$, obscures related signals for **9**). Anal. Calcd for $C_{35}H_{37}N_2O_2PdSbF_6$ ($\mathbf{12}_{(1,2)}$/$\mathbf{12}_{(2,1)}$): C, 48.89; H, 4.34; N, 3.26. Found: C, 48.29; H, 4.66; N, 3.06.

Preparation of [(N∧N)Pd(κ^2-C(Me)(Et)(OAc))][SbF_6] (13). A flame-dried Schlenk flask was charged with (N∧N)PdMeCl (162.7 mg, 0.300 mmol) and $AgSbF_6$ (97.1 mg, 2.83 mmol) in the drybox. Dry dichloromethane (20 mL) and vinylidene acetate (0.50 mL, 4.5 mmol) were precooled to −78 °C in a second flame-dried Schlenk flask. The dichloromethane solution was added to the solids by cannula transfer. The reaction was allowed to stir for ca. 10 min, and then the cold bath was removed and the reaction was allowed to warm to room temperature over the course of ca. 2 h. The solvent was removed in vacuo, and the product crystallized as brownish crystals from dichloromethane/ether at −30 °C (190.2 mg, 80% yield). ^{1}H NMR (CD_2Cl_2, 400 MHz): δ = 0.68 (dq, 1H, 7 Hz, 16 Hz $CH_3C\mathbf{H}$H′C(Me)(OAc)Pd), 1.00 (s, 3H, $C\mathbf{H_3}$CHH′C(Me)(OAc)Pd), 1.35 (t, 7.2 Hz, 3H, $C\mathbf{H_3}CH_2C$(Me)(OAc)-Pd), 1.50 (dq, 1H, 7 Hz, 16 Hz, $CH_3CH\mathbf{H}'$CH(OAc)Pd), 2.20 (s, 3H, $CO_2C\mathbf{H_3}$), 2.33 (s, 3H, Ar−$C\mathbf{H_3}$), 2.35 (s, 3H, Ar−$C\mathbf{H_3}$), 2.38 (s, 3H, Ar−$C\mathbf{H_3}$), 2.44 (s, 3H, Ar−$C\mathbf{H_3}$), 6.47, 6.86 (d, 6.8 Hz, 7.2 Hz, 1H each, H1 and H6 of acenaphthyl ligand), 7.3−7.5 (m, 6H, N−Ar signals), 7.60 (m, 2H, H2 and H5 of acenaphthyl ligand), 8.23, 8.26 (d, 8 Hz, 8.4 Hz, 1H each, H3 and H4 of acenaphthyl ligand). ^{13}C NMR (CD_2Cl_2, 100 MHz): 11.4 (Pd−C(Me)($CH_2\mathbf{C}H_3$)), 17.3, 17.6, 17.9, 18.0, (NAr−$\mathbf{C}H_3$ and $CO_2\mathbf{C}H_3$), 26.0 (PdCCH$_2$**Me**), 35.0 (Pd−C(Me)($\mathbf{C}H_2CH_3$), 118.1 (Pd−$\mathbf{C}$(Me)(Et)(OAc)), 124.5, 125.0, 125.5, 127.7, 127.8, 127.9, 128.8, 129.1, 129.2, 129.3, 129.4, 129.5, 129.6, 129.9, 130.0, 131.3, 132.9, 133.8, 142.4, 143.0, 146.1, 169.1, 175.7, 184.7 ($\mathbf{C}$=O).

Preparation of [(N∧N)Pd(κ^1-CH(Et)(OAc))(NCCH$_3$)][SbF_6] ($\mathbf{14}_\alpha$) and Isomers ($\mathbf{14}_\beta$ and $\mathbf{14}_\gamma$). A J. Young tube (Wilmad 504) was charged with [(N∧N)Pd(CH(Et)(OAc))][SbF_6] (**4b**) (35.3 mg, 42 μmol) and CD_2Cl_2 (500 μL). Acetonitrile (100 μL) was added under argon. ^{1}H NMR (CD_2Cl_2, 178 K, 500 MHz): δ = 0.52 (br. t, 3H, CH(OAc)-$CH_2C\mathbf{H_3}$); 1.14 and 1.49 (br. m, 1H each, CH(OAc)$C\mathbf{H_2}CH_3$); 1.73 (s,

3H, PdNCC**H**$_3$); 1.87, 2.13, 2.22, 2.25 (s, 3H each, N-aryl-C**H**$_3$); 2.37 (s, 3H, O_2CC**H**$_3$); 3.80 (br. d, 1H, 8.4 Hz, C**H**(OAc)(Et)); 6.51 and 6.94 (d, 1H each, 7.6, 7.2 Hz, acenaphthyl H3, H8); 7.21−7.33 (m, 6H, N−Aryl protons (*m* and *p*)); 7.48 and 7.52 (t, 1H each, 8.0 Hz, 7.6 Hz, acenaphthyl H4, H7); 8.15 and 8.18 (d, 1H each, 8.4 Hz, 8.8 Hz, acenaphthyl H5, H6). ^{13}C NMR (CD_2Cl_2, 178K, 125 MHz): δ = 2.2 (**C**H_3CN); 11.3 (CH(OAc)CH_2**C**H_3); 17.4, 17.4, 17.7, 17.9 (N−Aryl−**C**H_3); 21.0 (O_2C**C**H_3); 25.1 (CH(OAc)**C**H_2CH_3); 81.7 (**C**H(OAc)-CH_2CH_3); 124.4, 124.9, 126.8, 128.0, 128.3, 128.8, 128.8, 128.9, 129.1, 132.0, 132.8 (aromatic and acenaphthyl **C**−H carbons); 124.7, 127.0, 127.8, 127.9, 129.7, 130.2, 140.2, 141.7, 145.2, 167.5, 170.3, 174.3 (quaternary aromatic and acenaphthyl carbons) 186.5 (O_2**C**CH_3). CH_3**C**N−Pd obscured by free CH_3CN. Upon warming the above solution of **14**$_\alpha$, signals assigned by COSY to **14**$_\beta$ and **14**$_\gamma$ were observed. ^{1}H NMR (500 MHz, COSY, 265 K) **14**$_\beta$: 4.02, 3.47 (CH(Me)C**H**$_2$), 1.60 (C**H**(Me)CH_2), 0.70 (CH(**Me**)CH_2). **14**$_\gamma$: 3.88 (PdCH_2CH_2C**H**$_2$OAc), 1.28 (PdCH_2C**H**$_2CH_2$OAc), 1.57 (PdC**H**$_2CH_2$-CH_2OAc).

Preparation of [(N∧N)Pd(κ^1-C(O)CH(Et)(OAc))(NCCH_3)][SbF_6] (15$_\alpha$) and Isomers (15$_\beta$ and 15$_\gamma$). Initially using the same procedure described for**14**$_{\alpha-\gamma}$, a sample was subsequently freeze−pump−thawed and placed under an atmosphere of CO to generate **15**$_{\alpha-\gamma}$. ^{1}H NMR (COSY, 500 MHz, 293 K) **15**$_\alpha$: 0.70 (PdC(O)CH(OAc)CH_2C**H**$_3$), 1.32, 1.74(PdC(O)CH(OAc)C**H**$_2CH_3$), 4.98 (PdC(O)C**H**(OAc)CH_2CH_3). **15**$_\beta$: 0.96 (PdC(O)CH(C**H**$_3$)CH_2OAc), 3.07 (PdC(O)C**H**(CH_3)CH_2OAc), 3.94 (PdC(O)CH(CH_3)C**H**$_2$OAc). **15**$_\gamma$: 3.69 (PdC(O)CH_2CH_2C**H**$_2$OAc), 1.46 (PdC(O)CH_2C**H**$_2CH_2$OAc), 2.82 (PdC(O)C**H**$_2CH_2CH_2$OAc).

Partial NMR Data for 16−18. ^{1}H NMR for **16** (158 K, $CDCl_2F$, 500 MHz): All signals extremely broad. 4.94 (2H, CH_2C**H**$_2$), 4.31 (1H, C**H**HCH_2), 4.22 (1H, CH**H**CH_2), 4.12 (1H, PdC**H**(OAc)CH_2CH_3), 1.63 (1H, PdCH(OAc)C**H**HCH_3-other methylene proton obscured), 0.33 (3H, PdCH(OAc)CH_2C**H**$_3$). ^{1}H NMR for **17** (233 K, CD_2Cl_2, 500 MHz): 4.07 (1H, PdC**H**(OAc_f)CH_2CH_3), 1.71 (1H, PdCH(OAc_f)C**H**HCH_3), 1.34 (1H, PdCH(OAc)CH**H**CH_3), 0.67 (3H, PdCH(OAc_f)CH_2C**H**$_3$). ^{1}H NMR for **18** (233 K, CD_2Cl_2, 500 MHz): 4.71 (4H, AB pattern, C**H**$_2$C**H**$_2$), 4.28 (1H, PdC**H**(OAc_f)CH_2CH_3), 1.89 (1H, PdCH(OAc_f)-C**H**HCH_3), 1.68 (1H, PdCH(OAc)CH**H**CH_3), 0.35 (3H, PdCH(OAc_f)-CH_2C**H**$_3$).

Thermolysis Experiments (General Procedure). In thermolysis experiments of **4a**, **4b**, **11**$_{(2,1)}$, **11**$_{(1,2)}$, **12**$_{(2,1)}$, **12**$_{(1,2)}$, and **13**, a small amount of the complex (8−20 mg) was added to a J. Young NMR tube charged with $CDCl_2CDCl_2$ (ca. 300 μL) while in an argon-filled glovebox. Kinetic experiments were carried out in the NMR probe (temperature calibrated with ethylene glycol), and reactions were monitored by the disappearance of integration intensity of the terminal methyl signal on the alkyl chain attached to the acetate moiety. For **6**, an NMR tube was charged in the glovebox with **6** and capped with a septum. Outside the glovebox, the NMR tube was cooled in dry ice/acetone, and dry CD_2Cl_2 was added through the septum via gastight syringe. The tube was placed in the NMR probe while cold (<−40 °C), and the NMR probe was then warmed to −10 °C and the reaction was monitored as described above. Low-temperature calibration was performed with a methanol standard in place of ethylene glycol.

Insertion Kintetics (General Procedure). Samples were prepared as described above for low-temperature kinetics of **6**, with either CD_2Cl_2 or $CDCl_2F$ as the solvent. The probe was precooled to −80 °C before adding the sample and was then warmed to the temperature at which the kinetic experiment was performed.

Ethylene Insertion into Pd−C Bond of 16. Standard kinetic NMR procedures were followed with the following modifications. Spectra were acquired at −40 °C, while the reaction was allowed to proceed at 0° in an ice bath between spectra. Ethylene (2−10 mL at 25 °C) was syringed into the solution at varying intervals to maintain a pressure of ethylene in the tube. During ethylene addition, the tube was maintained at −78 °C and shaken vigorously in order to adequately dissolve the ethylene. As ethylene consumption increased in rate as the reaction progressed, it was only possible to monitor the reaction at very early reaction times. Propylene was not observed under these circumstances, and signals between 0.9 and 1.4 ppm grew in with time, suggesting the growth of a polyethylene chain.

Acknowledgment. The authors thank Mr. Weijun Liu for his determination of the relative binding constants of ethylene and *para*-vinyl anisole and Professor Olafs Daugulis for many helpful discussions. The authors also thank the National Science Foundation(CHE-0107810) and DuPont for financial support of this work.

Supporting Information Available: Crystallographic data for **4b** as a CIF file. This material is available free of charge via the Internet at http://pubs.acs.org.

JA045969S